NATIONAL ADVISORY COMMITTEE FOR AERONAUTICS

TECHNICAL NOTE 3967

CHARACTERISTICS OF A 40° CONE FOR MEASURING MACH NUMBER, TOTAL PRESSURE, AND FLOW ANGLES AT SUPERSONIC SPEEDS

By Frank J. Centolanzi

Ames Aeronautical Laboratory
Moffett Field, Calif.

Washington
May 1957

NATIONAL ADVISORY COMMITTEE FOR AERONAUTICS

TECHNICAL NOTE 3967

CHARACTERISTICS OF A 40° CONE FOR MEASURING MACH NUMBER, TOTAL PRESSURE, AND FLOW ANGLES AT SUPERSONIC SPEEDS

By Frank J. Centolanzi

SUMMARY

An experimental investigation was conducted to determine the characteristics of a 40° cone for use in the measurement of Mach number, total pressure, and flow angles. The cone had a total-pressure orifice at the apex and four equally spaced static-pressure orifices on the surface. Pressure measurements were taken at angles of pitch up to 26° at Mach numbers of 1.72, 1.95, and 2.46 for Reynolds numbers of 3.12 and 5.41 million per foot. This instrument is capable of measuring Mach number within approximately ±1.0 percent and the flow angles within ±0.25°. The total pressure can be measured within ±0.5 percent at a Mach number of 1.72 and within ±2.0 percent at a Mach number of 2.46. These flow quantities can be determined from the measured cone pressures and charts presented in this report. In general, an iterative procedure is required; however, in practice, such a procedure is necessary only for accurate determination of the Mach number and total pressure at Mach numbers near 2.5.

INTRODUCTION

An instrument which is capable of measuring Mach number, total pressure, and flow angles simultaneously is of considerable value for both flight and wind-tunnel applications. One type of instrument suitable for this purpose is described in references 1, 2, and 3 and consists of a cone with four equally spaced static-pressure orifices on the surface and a total-pressure orifice at the apex. However, the existing experimental data for such instruments are restricted to low supersonic or subsonic Mach numbers and, in most cases, to small flow angles. Because of the need for data over a wider range of Mach number and flow angles on instruments of this type, the present investigation was undertaken. The characteristics of five identical 40° included-angle cones were determined experimentally at Mach numbers of 1.72, 1.95, and 2.46 for angles of pitch up to 26°.

SYMBOLS

C_p surface pressure coefficient, $\frac{p_s - p_1}{q_1}$

$\left(\frac{\Delta p}{q_1}\right)_\epsilon$ difference in pressure coefficient between orifices c and a, $\frac{p_{s_c} - p_{s_a}}{q_1}$ (fig. 2)

$\left(\frac{\Delta p}{q_1}\right)_\sigma$ difference in pressure coefficient between orifices d and b, $\frac{p_{s_d} - p_{s_b}}{q_1}$ (fig. 2)

p_{t_2} pitot pressure measured behind normal shock wave at cone apex

p_{t_1} total pressure ahead of normal shock wave at cone apex

M_1 Mach number ahead of normal shock wave at cone apex

p_s static pressure on cone surface

p_1 static pressure ahead of normal shock wave at cone apex

$\bar{p}_A$ arithmetic mean of four static pressures, $\frac{1}{4}\left(p_{s_a} + p_{s_b} + p_{s_c} + p_{s_d}\right)$

q_1 dynamic pressure ahead of normal shock wave at cone apex

u_1, v_1, w_1 velocities in X, Y, Z directions (fig. 2)

V_1 velocity ahead of normal shock wave at cone apex

X, Y, Z Cartesian coordinates of body axes (fig. 2)

α angle of attack, deg (fig. 2)

β angle of sideslip, deg (fig. 2)

ϵ angle of downwash, deg (fig. 2)

θ angle of pitch of cone axis, deg (fig. 2)

σ angle of sidewash, deg (fig. 2)

φ	angle of roll, deg (fig. 2)

Subscripts

1	conditions ahead of normal shock wave at apex of cone
2	conditions behind normal shock wave at apex of cone
a,b,c,d	position of orifices on cone surface (fig. 2)
θ	quantity at angle of pitch
θ=0	quantity at zero angle of pitch

MODELS AND APPARATUS

Wind Tunnel

The Ames 1- by 3-foot supersonic wind tunnel No. 1 is a single return, variable-pressure wind tunnel having a Mach number range at the time of these tests of 1.4 to 2.5. The Mach number is changed by varying the contour of flexible plates which comprise the top and bottom walls of the tunnel.

Models and Support

The test models were cone-cylinder combinations utilizing cones with an included angle of 40°. The cones were constructed of stainless steel within decimal tolerances of ±0.001 inch and angular tolerances of ±5 minutes. There were four equally spaced static-pressure orifices on the surface of each cone and a total-pressure orifice at each apex. The details of the model and support are shown in figure 1. An included angle of 40° was chosen as a compromise between the following considerations:

1. It is desirable to use a cone with as large an included angle as possible to delay flow separation to large flow angles.

2. A cone with a large included angle has a greater pressure difference across two diametrically opposed orifices at given flow angles than a slender cone and thus is more sensitive.

3. For flow-field surveys in wind tunnels it is desirable to minimize the disturbance created by the cone. From this consideration a small included angle would be desirable.

The lip at the entry of the total-pressure orifice was made sharp (0.002 inch thick) because the data of reference 4 indicate that sharp lips extend the range of flow angles through which the pitot pressure remains constant.

Five 40° cones were attached to a wedge-shaped strut which projected from the side wall of the tunnel as shown in figure 1. The strut could be pitched about an axis which passed through the station of the static-pressure orifices of the cones, but it could not be yawed in the wind tunnel. In order to obtain various combinations of downwash and sidewash relative to the cones, they were rolled about their longitudinal axes. This arrangement also minimized any errors due to the longitudinal pressure gradient in the wind tunnel.

PRECISION OF THE RESULTS

The estimated uncertainty in the experimental results at all Mach numbers is given in the following table:

Quantity	Uncertainty
C_p	±0.005
$\bar{p}_A/p_{t_2}$	±.003
θ	±.10°
φ	±.10°
M_1	±.005

For instruments of identical geometry connected to pressure-sensing elements comparable to those used in this investigation (see uncertainties for C_p and $\bar{p}_A/p_{t_2}$), the precision with which local flow quantities can be determined by means of the procedures described in this report is estimated to be as follows:

	Precision		
	$M_1 = 1.72$	$M_1 = 1.95$	$M_1 = 2.46$
M_1	±0.01	±0.015	±0.03
p_{t_1}	±.5%	±1.0%	±2.0%
ϵ	±.25°	±.25°	±.25°
σ	±.25°	±.25°	±.25°

TESTS

Tests were conducted at Mach numbers of 1.72, 1.95, and 2.46 for two values of Reynolds number: 3.12 and 5.41 million per foot. At each Mach number, for the lower Reynolds number, the cones were set at roll angles from -90° to $+90^\circ$ in 10° increments and pitched through as large an angle range as possible in both the positive and negative directions (see fig. 2). The maximum range at each Mach number was restricted by interference effects from the support system. In addition, tests were made through the angle-of-pitch range at a roll angle of 45° for both Reynolds numbers.

RESULTS AND DISCUSSION

A comparison of the results showed no difference from cone to cone and no effect of Reynolds number. For this reason, the results for one typical cone will be presented for a Reynolds number of 3.12×10^6 per foot.

Charts are presented which enable the determination of Mach number, total pressure, and flow angles. A numerical example is presented in the Appendix which illustrates the procedure for determining these quantities.

Cone Pressure Distribution

The pressure distribution on the surface of the cone is shown in figure 3 for the three test Mach numbers and various angles of pitch. Because the cone apex angle is relatively large, the pressure coefficients over the entire surface are positive throughout the angle-of-pitch range tested except at the largest angle of pitch for $M = 2.46$, where a small region of negative pressure coefficients exists on the leeward surface. Representative experimental results of figure 3 are compared in figure 4 with the pressure distributions given by the theoretical method of references 6 and 7. In the use of these references it is necessary to employ constants tabulated in reference 5. The first-order nonlinear theory of reference 6 provides a reasonably good prediction of the pressures only near the side of the cone ($\varphi = 90^\circ$) but gives considerably more negative pressure coefficients near the top and bottom of the cone. The second-order theory of reference 7, on the other hand, gives a good approximation to the variation of the pressures over the entire surface.

In reference 8 Ferri has shown that the theory of references 6 and 7 is based on an incorrect distribution of entropy at the surface of the cone. However, the results of reference 9 indicate that the numerical effect of this error on the pressures is negligible and could not account for the differences shown in the comparisons of figure 4.

Determination of Mach Number

The determination of Mach number by a conical pitot-static tube depends on the ratio of a surface static pressure to the pitot pressure and on the flow inclination (angles of pitch and roll). At zero angle of pitch the Mach number can be computed from the ratio of the static pressure to the pitot pressure. Experimental results for this condition are shown in figure 5. The values of the Mach number for this figure were obtained from the measured ratio of the pitot pressure to the total pressure p_{t_2}/p_{t_1} using the theoretical normal shock-wave relations. Comparison with the theory of reference 5 shows satisfactory agreement only near $M_1 = 1.72$.

At angles of pitch, large variations in the static pressure occur around the circumference of the cone as previously shown in figure 3. It is desirable to combine the four measured pressures on the cone surface in such a manner as to provide a pressure which is essentially invariant to changes in angle of pitch. The results of references 1 and 2, which were restricted to Mach numbers near 1.60, indicate that for low angles of pitch the arithmetic average of the four static pressures is nearly constant. Similar results were obtained in the present investigation. Figure 6 shows the variation of the ratio of the arithmetically averaged static pressures to the pitot pressure $\bar{p}_A/p_{t_2}$ with pitch angle θ. The data from test runs with geometrically similar roll angles were averaged as, for example, the data for test runs with $\varphi = +10^\circ$, -10°, $+80^\circ$, and -80°, because the averaged static pressures would be expected to be the same from reasons of symmetry.

In general, the procedure for determining Mach number is first to assume that $\theta = 0$. A first approximation to the Mach number is then obtained from figure 5 for the measured value of $\bar{p}_A/p_{t_2}$. The flow angles, θ and φ, are then determined by the method described in the section "Determination of Flow Angles." When θ and φ are known, a correction factor for $\bar{p}_A/p_{t_2}$ is obtained from figure 6 and an equivalent value of $\bar{p}_A/p_{t_2}$ corresponding to $\theta = 0$ is calculated by a division of the measured value by this correction factor. A second approximation to the Mach number is obtained from figure 5. In principle, this process is then repeated to obtain a close approximation to the true Mach number. In practice, however, because of the small dependence of $\bar{p}_A/p_{t_2}$ on θ and φ (fig. 6), the first approximation is sufficient except for Mach numbers of the order of 2.5 with θ greater than about 10° in which case only one iteration is normally required.

The error in measuring the Mach number with the use of figures 5 and 6 is estimated to be ± 0.01 at $M_1 = 1.72$, ± 0.015 at $M_1 = 1.95$, and ± 0.03 at $M_1 = 2.46$.

Determination of Total Pressure

The total pressure is a function of the pitot pressure, Mach number, and the angle of pitch. The results of tests reported in reference 4 for a wide variety of pitot tubes have shown that at zero angle of pitch the ratio of the pitot pressure to the total pressure at any supersonic Mach number is equal to the theoretical total-pressure ratio across a normal shock wave. This result is assumed to apply to the cone of the present investigation.

The effect of angle of pitch on the measured pitot pressure is shown in figure 7. It is observed that this effect is negligible over a large angle range (approximately $\pm 25^{\circ}$) and is independent of the test Mach numbers for angles of pitch less than 25°. The total pressure at a given Mach number, p_{t_1}, is obtained by dividing the measured pitot pressure, p_{t_2}, by the ratio of the pitot pressure to the total pressure across a normal shock wave, p_{t_2}/p_{t_1}. For angles above 25° the measured pitot pressure must first be divided by the appropriate factor from the calibration shown in figure 7 in order to obtain an equivalent value at $\theta = 0$.

The estimated error in measuring the total pressure p_{t_1} depends primarily upon the Mach number error. The percent error in measuring the total pressure is estimated to be ± 0.5 percent at $M_1 = 1.72$, ± 1.0 percent at $M_1 = 1.95$, and ± 2.0 percent at $M_1 = 2.46$.

Determination of Flow Angles

The flow angles can be determined from the pressure differences across the sets of diametrically opposed orifices. The variation of the difference in static pressure coefficient across opposed orifices is presented in figure 8 for the various Mach numbers. The dynamic pressure is determined from the total pressure and the Mach number. Because of wind-tunnel stream angle and support misalignment, the curves do not pass through the origin.

In order to facilitate the determination of θ and φ from measurements of $(\Delta p/q_1)_{\epsilon}$ and $(\Delta p/q_1)_{\sigma}$, the results of figure 8 have been combined in figure 9 to give plots of $(\Delta p/q_1)_{\epsilon}$ versus $(\Delta p/q_1)_{\sigma}$ for various θ and φ. Each curve of figure 8 was first shifted through the origin to eliminate the effects of tunnel stream angle and support misalignment. Because of symmetry, curves which represent an average of the data in the four quadrants are shown in one quadrant only. Information for the other quadrants, then, can be determined from this figure provided the proper sign convention is used as indicated. Comparisons among figures 9(a), 9(b), and 9(c) show that the effects of Mach number are either negligible or small. The flow inclination in terms of ϵ and σ can be calculated from θ and φ by the following relations:

$$\tan \epsilon = -\tan \theta \cos \varphi$$
$$\tan \sigma = \tan \theta \sin \varphi$$

For convenience in obtaining the quantities directly, curves are presented in figure 10 from which these angles can be determined without recourse to the equations. The sign conventions for quadrants other than that shown are indicated in the figure. Any correction to the Mach number results in a corresponding change in the dynamic pressure, but only a small correction in the flow angle is required.

The error in measuring flow angles is estimated to be $\pm 0.25^\circ$.

In cases where this instrument is to be used to measure the attitude of an aircraft in flight or in a wind tunnel, the angles of attack and sideslip can be calculated from θ and φ (fig. 9) by the following expressions:

$$\tan \alpha = \tan \theta \cos \varphi$$
$$\sin \beta = -\sin \theta \sin \varphi$$

CONCLUDING REMARKS

The characteristics of a 40° cone for measuring Mach number, total pressure, and flow angles were determined experimentally. Tests were conducted at Mach numbers of 1.72, 1.95, and 2.46 for angles of pitch up to 26°. This instrument is capable of measuring Mach number within approximately ± 1.0 percent and the flow angles within $\pm 0.25^\circ$. The total pressure can be measured within ± 0.5 percent at a Mach number of 1.72 and within ± 2.0 percent at a Mach number of 2.46. These flow quantities can be determined from the measured cone pressures and calibration charts of this investigation. In general an iterative procedure is required; however, in practice, such a procedure is necessary only for accurate determination of the Mach number and total pressure at Mach numbers near 2.5.

Ames Aeronautical Laboratory
National Advisory Committee for Aeronautics
Moffett Field, Calif., Mar. 1, 1957

APPENDIX

NUMERICAL EXAMPLE

The procedure used in determining the Mach number, total pressure, and flow direction from the measured pitot pressure and four static pressures on the cone surface is illustrated by the following numerical example. The assumed pressures are:

$$p_{s_a} = 1.10 \text{ psia}$$
$$p_{s_b} = 1.20 \text{ psia}$$
$$p_{s_c} = 3.85 \text{ psia}$$
$$p_{s_d} = 2.90 \text{ psia}$$
$$p_{t_2} = 7.65 \text{ psia}$$

The arithmetic mean of the four static pressures is

$$\bar{p}_A = \frac{1}{4}\left(p_{s_a} + p_{s_b} + p_{s_c} + p_{s_d}\right) = 2.26 \text{ psia}$$

and the ratio of this static pressure to the pitot pressure is

$$\frac{\bar{p}_A}{p_{t_2}} = 0.295$$

If it is first assumed that $\theta = 0$, a tentative Mach number of 2.36 is obtained from figure 5. For $\theta = 0$, the total pressure ratio p_{t_2}/p_{t_1} is given by the theoretical normal shock-wave relations which are tabulated in reference 10. For $M_1 = 2.36$ this ratio is

$$\frac{p_{t_2}}{p_{t_1}} = 0.5572$$

and the total pressure p_{t_1} is

$$p_{t_1} = \frac{\left(p_{t_2}\right)_\theta}{\left(p_{t_2}/p_{t_1}\right)_{\theta=0}} = \frac{7.65}{0.5572} = 13.73 \text{ psia}$$

The dynamic pressure q_1 is given by

$$q_1 = \left(q_1/p_{t_1}\right)p_{t_1} = 0.2839(13.73) = 3.90 \text{ psia}$$

where the quantity q_1/p_{t_1} is given by the theoretical isentropic flow relations also tabulated in reference 10. Dividing the pressure difference across both pairs of orifices by the dynamic pressure gives

$$\left(\frac{\Delta p}{q_1}\right)_\epsilon = \frac{p_{s_c} - p_{s_a}}{q_1} = \frac{3.85 - 1.10}{3.90} = 0.705$$

$$\left(\frac{\Delta p}{q_1}\right)_\sigma = \frac{p_{s_d} - p_{s_b}}{q_1} = \frac{2.90 - 1.20}{3.90} = 0.436$$

The downwash and sidewash angles from figure 10(c) are $\epsilon = -16.9^\circ$ and $\sigma = 10.3^\circ$. Now, in order to correct the Mach number, the angles of pitch and roll must be known. From figure 9(c) $\theta = 19.6^\circ$ and $\varphi = 30.5^\circ$. The correction factor from figure 6(c) is

$$\frac{\left(\bar{p}_A/p_{t_2}\right)_\theta}{\left(\bar{p}_A/p_{t_2}\right)_{\theta=0}} = 1.05$$

The corrected value of $\bar{p}_A/p_{t_2}$ corresponding to $\theta = 0$ is

$$\frac{\bar{p}_A}{p_{t_2}} = \frac{\left(\bar{p}_A/p_{t_2}\right)_\theta}{\left(\bar{p}_A/p_{t_2}\right)_\theta / \left(\bar{p}_A/p_{t_2}\right)_{\theta=0}} = \frac{0.295}{1.05} = 0.281$$

From figure 5 the second approximation to the Mach number is $M_1 = 2.48$. Using this new value of Mach number gives

$$\frac{p_{t_2}}{p_{t_1}} = 0.5071$$

Since the angle of pitch is less than 25°, the pitot pressure need not be corrected to an equivalent value at $\theta = 0$. The second approximation to the total pressure is

$$p_{t_1} = \frac{7.65}{0.5071} = 15.08 \text{ psia}$$

and the dynamic pressure is $q_1 = 0.2599(15.08) = 3.92$ psia. Since the second determination of the dynamic pressure is essentially the same as the first, the angles of pitch and roll need no correction. Repeated iteration would be unnecessary since the correction factors of figure 6 would be unchanged.

REFERENCES

1. Cooper, Morton, and Webster, Robert A.: The Use of an Uncalibrated Cone for Determination of Flow Angles and Mach Numbers at Supersonic Speeds. NACA TN 2190, 1951.

2. Davis, Theodore: Development and Calibration of Two Conical Yawmeters. Meteor Rep. UAC-43, United Aircraft Corp., Oct. 1949.

3. Raney, D. J.: Flow Direction Measurements in Supersonic Wind Tunnels. R.A.E. TN Aero. 2342, Sept. 1954.

4. Gracey, William, Colletti, Donald E., and Russell, Walter R.: Wind-Tunnel Investigation of a Number of Total-Pressure Tubes at High Angles of Attack. NACA TN 2261, 1951.

5. Staff of the Computing Section, (under the direction of Zdeněk Kopal): Tables of Supersonic Flow Around Cones. Tech. Rep. No. 1, Center of Analysis, M.I.T., 1947.

6. Staff of the Computing Section, (under the direction of Zdeněk Kopal): Tables of Supersonic Flow Around Yawing Cones. Tech. Rep. No. 3, Center of Analysis, M.I.T., 1947.

7. Staff of the Computing Section, (under the direction of Zdeněk Kopal): Tables of Supersonic Flow Around Cones of Large Yaw. Tech. Rep. No. 5, Center of Analysis, M.I.T., 1947.

8. Ferri, Antonio: Supersonic Flow Around Circular Cones at Angles of Attack. NACA TN 2236, 1950.

9. Roberts, Richard C., and Riley, James D.: A Guide to the Use of the M.I.T. Cone Tables. Navord Rep. 2606, Apr. 1, 1953.

10. Ames Research Staff: Equations, Tables and Charts for Compressible Flow. NACA Rep. 1135, 1953.

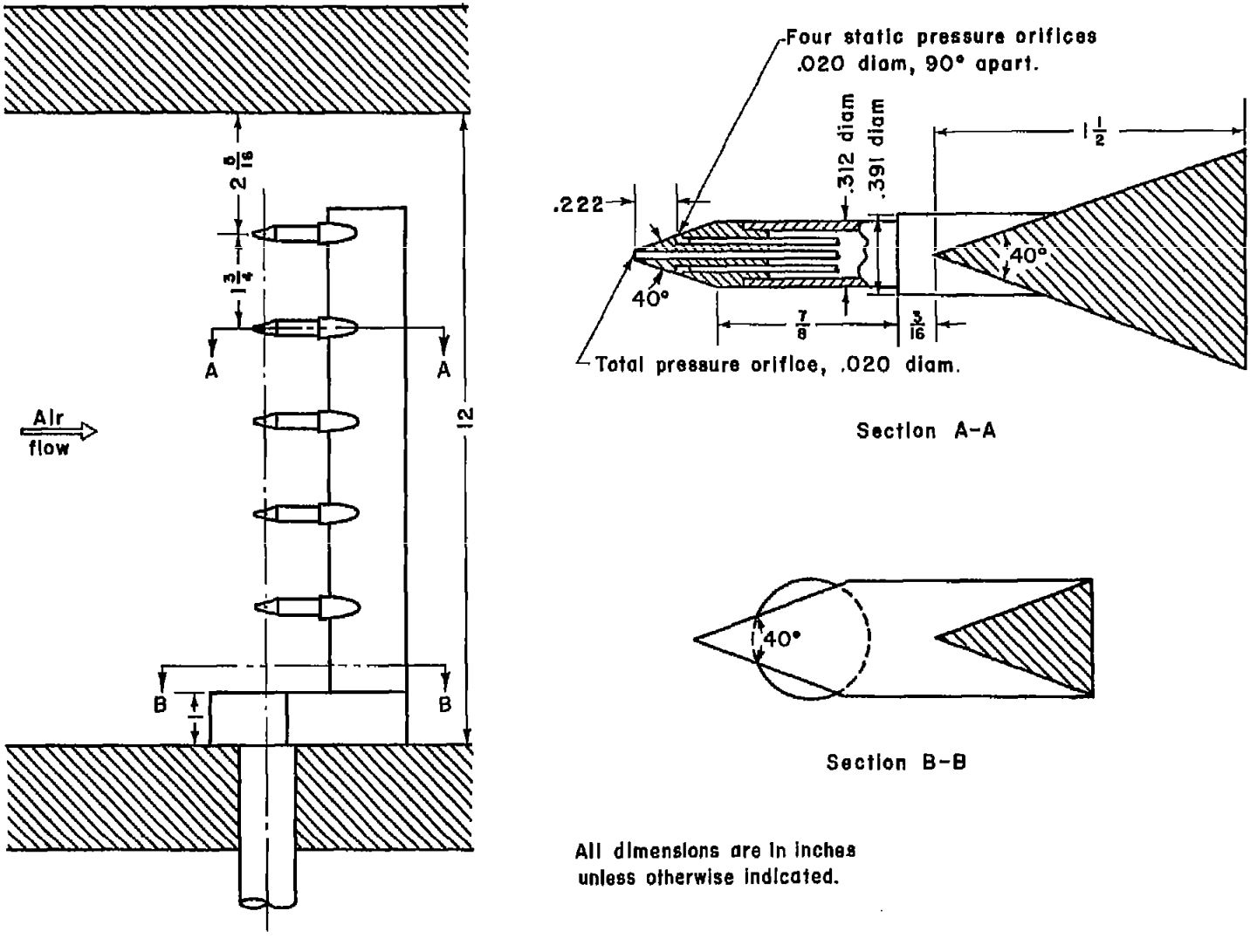

Figure 1.—Models and support.

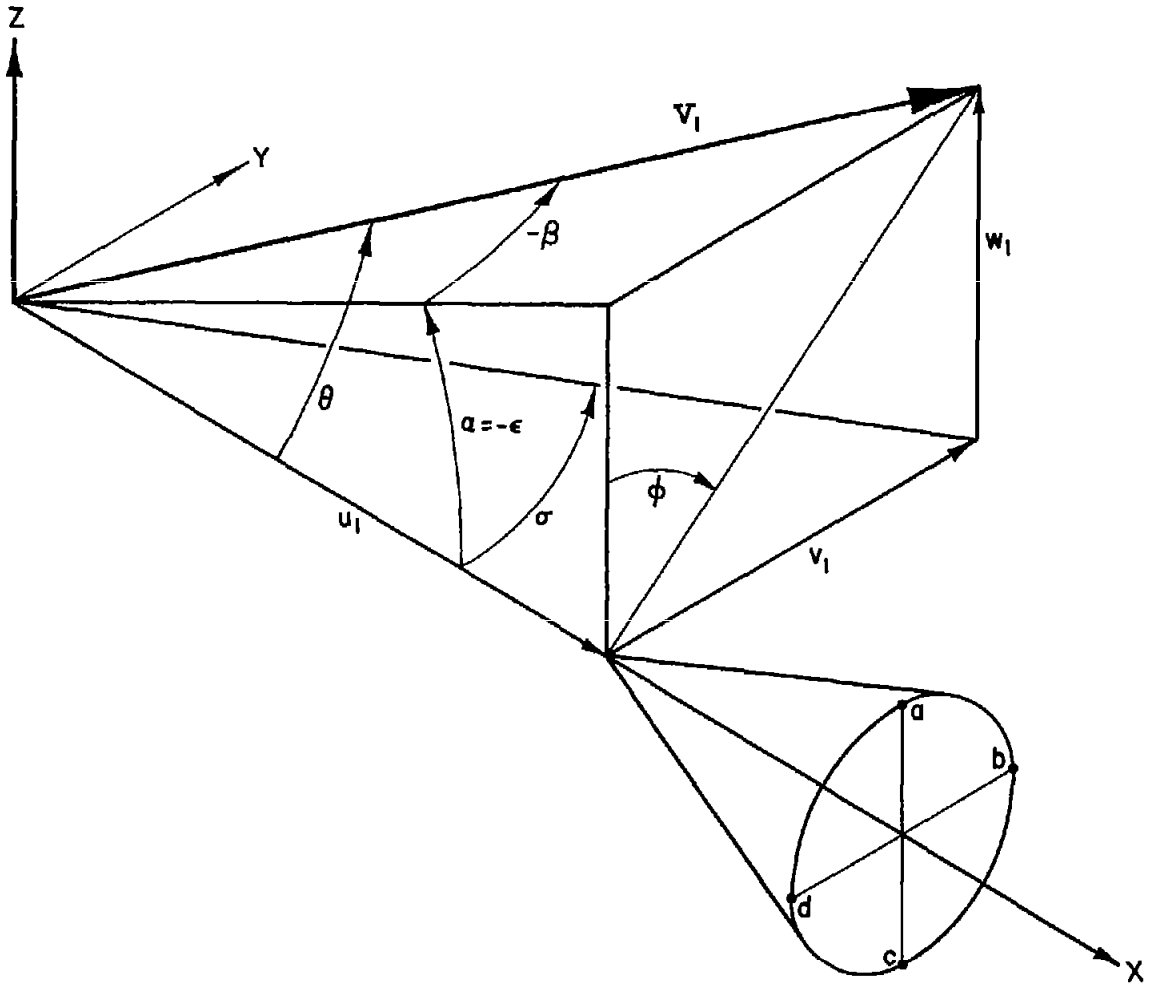

Figure 2.– Orifice designation and angle notation.

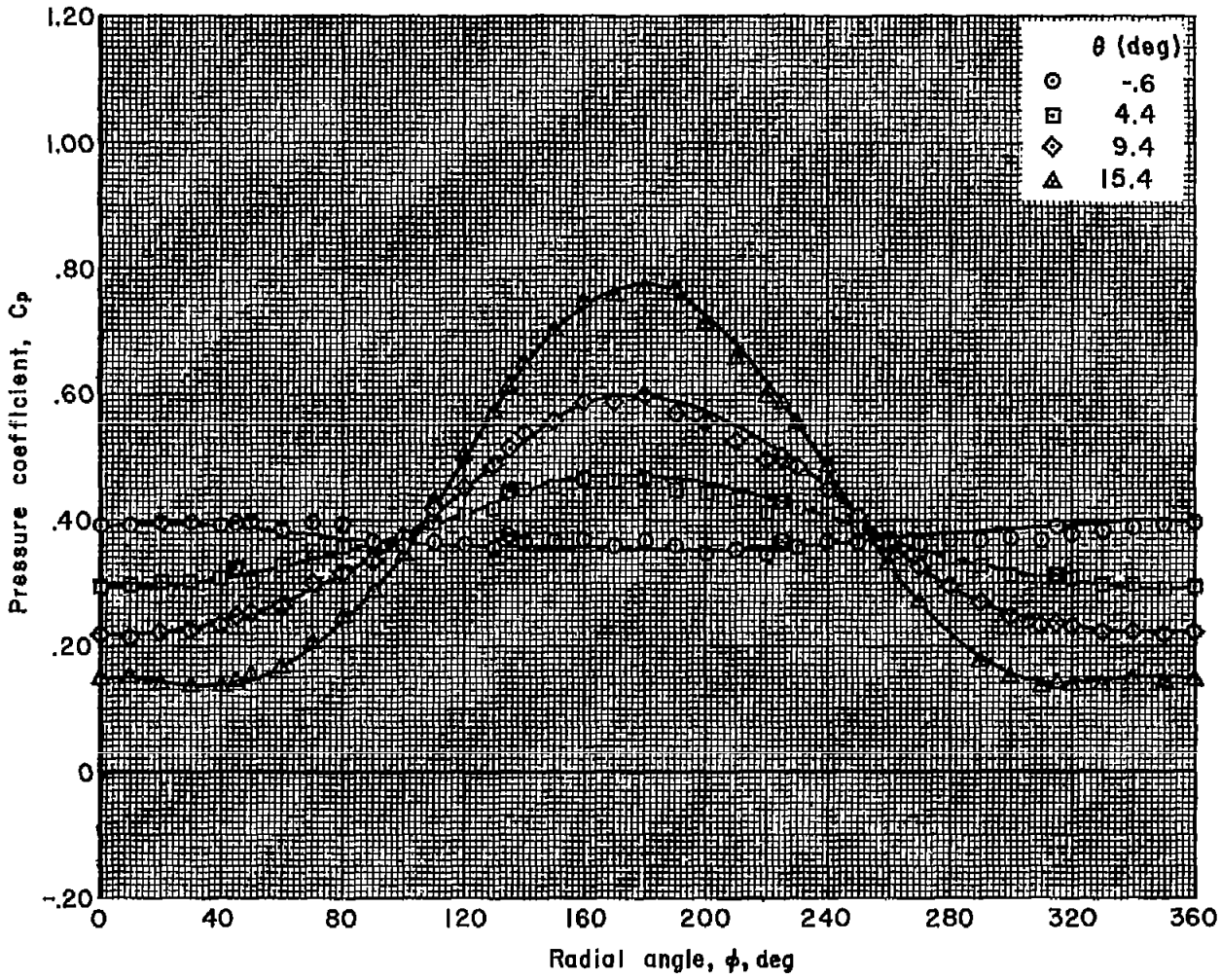

(a) $M_1 = 1.72$

Figure 3.—Circumferential pressure distribution on surface of cone.

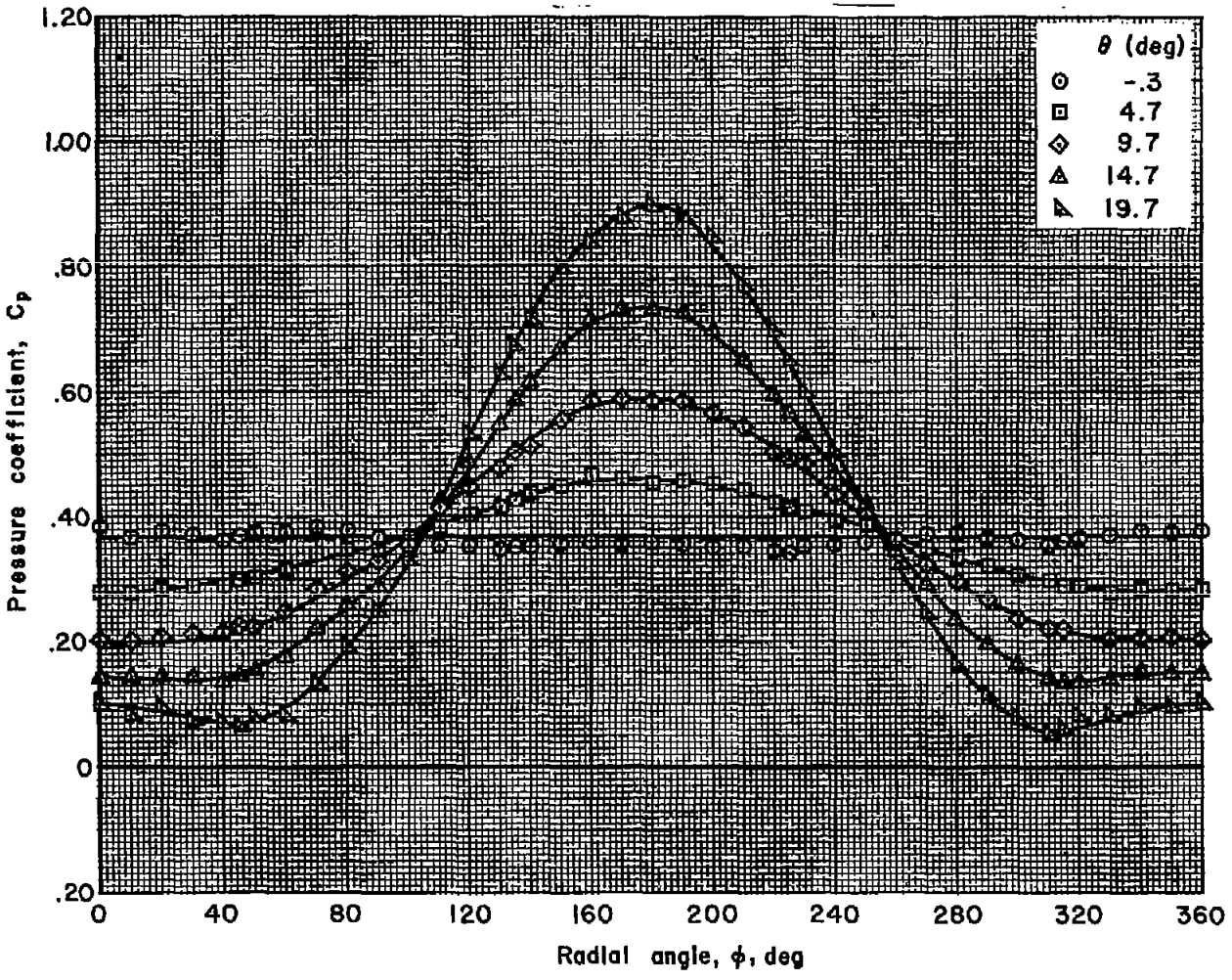

(b) M_1=1.95

Figure 3.–Continued.

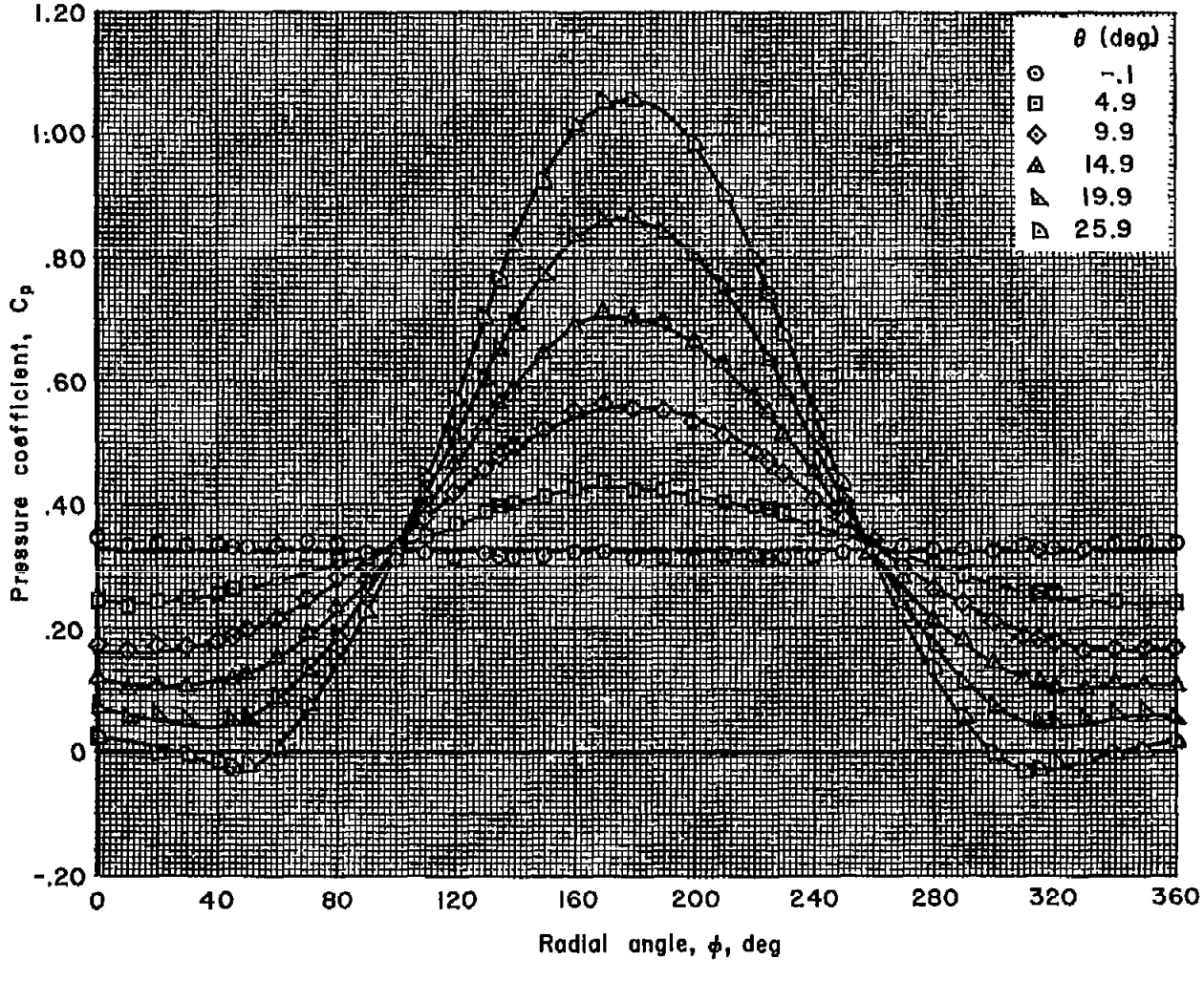

(c) M_1=2.46

Figure 3.- Concluded.

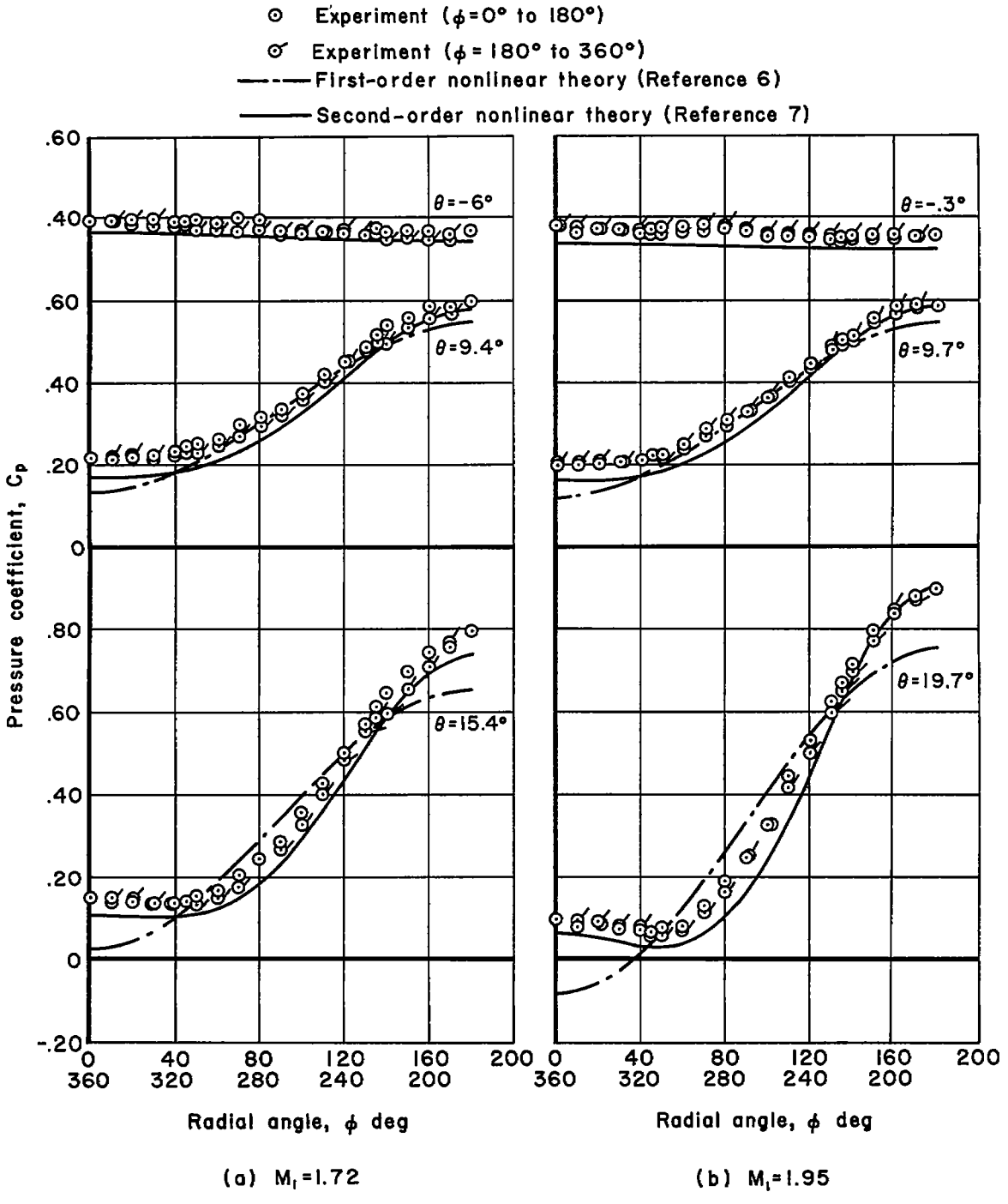

Figure 4.—Comparison of experimental and theoretical pressure distributions on surface of cone.

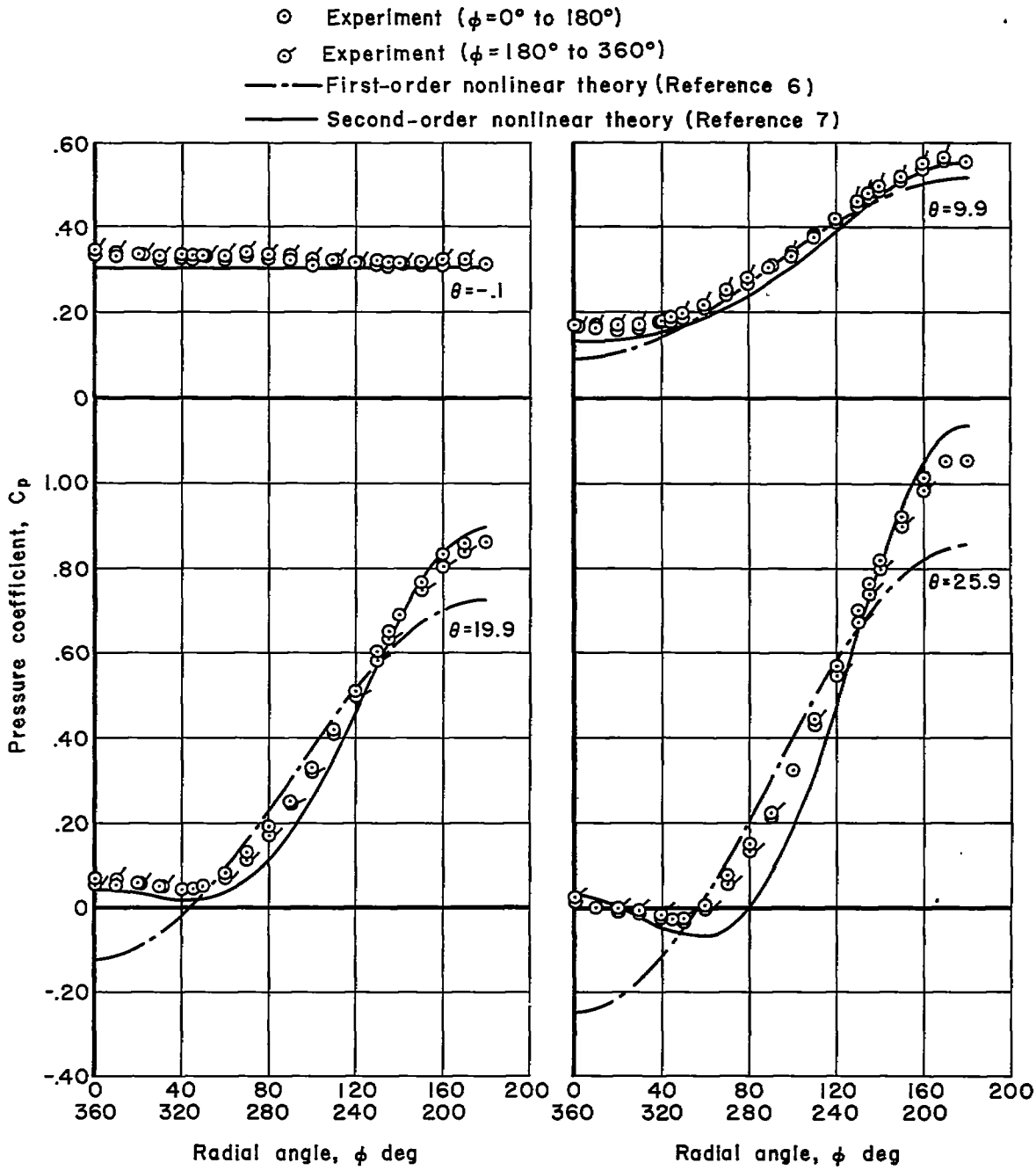

(c) $M_1 = 2.46$

Figure 4.- Concluded.

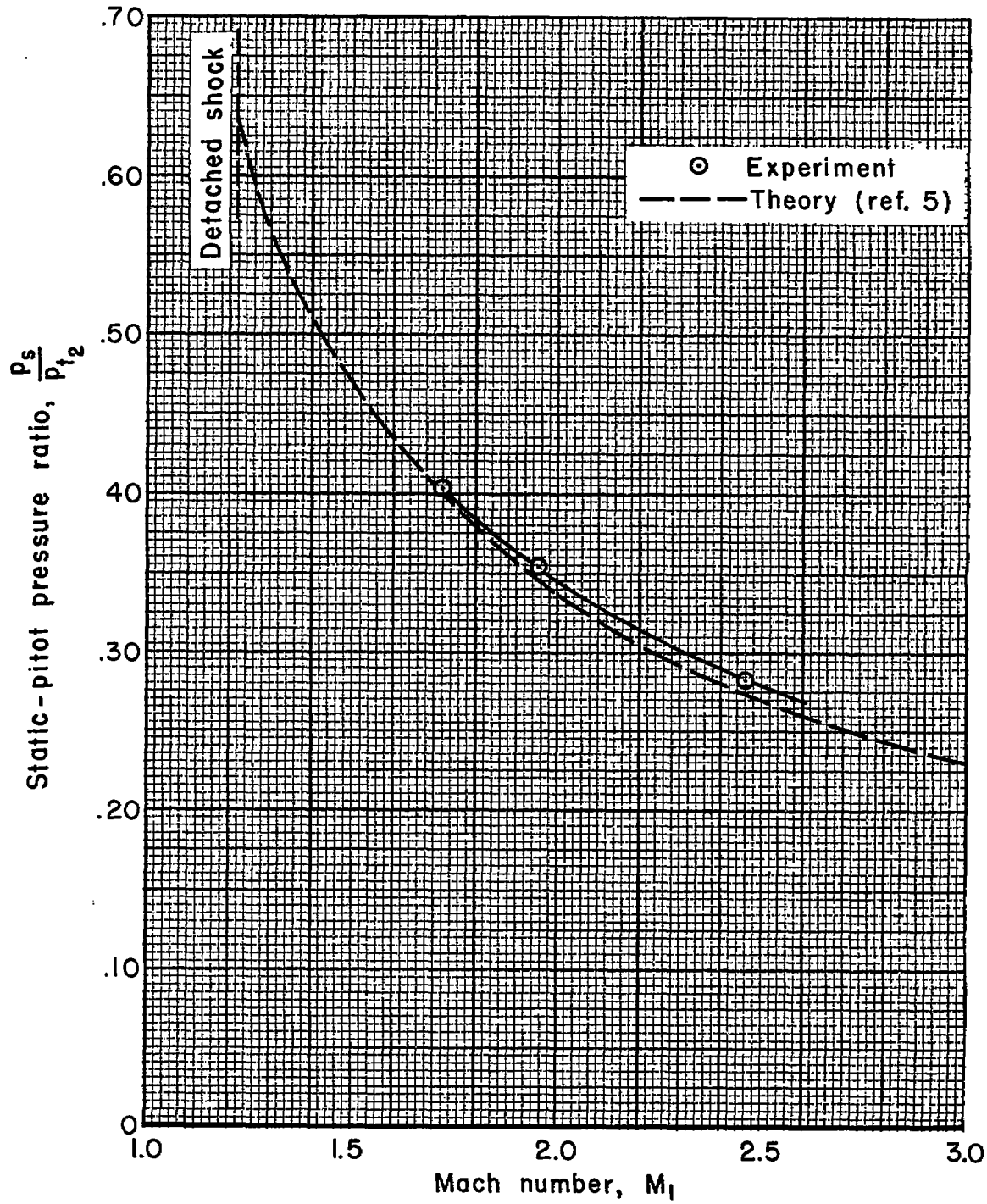

Figure 5.– Variation of static-pitot pressure ratio with Mach number at zero angle of pitch

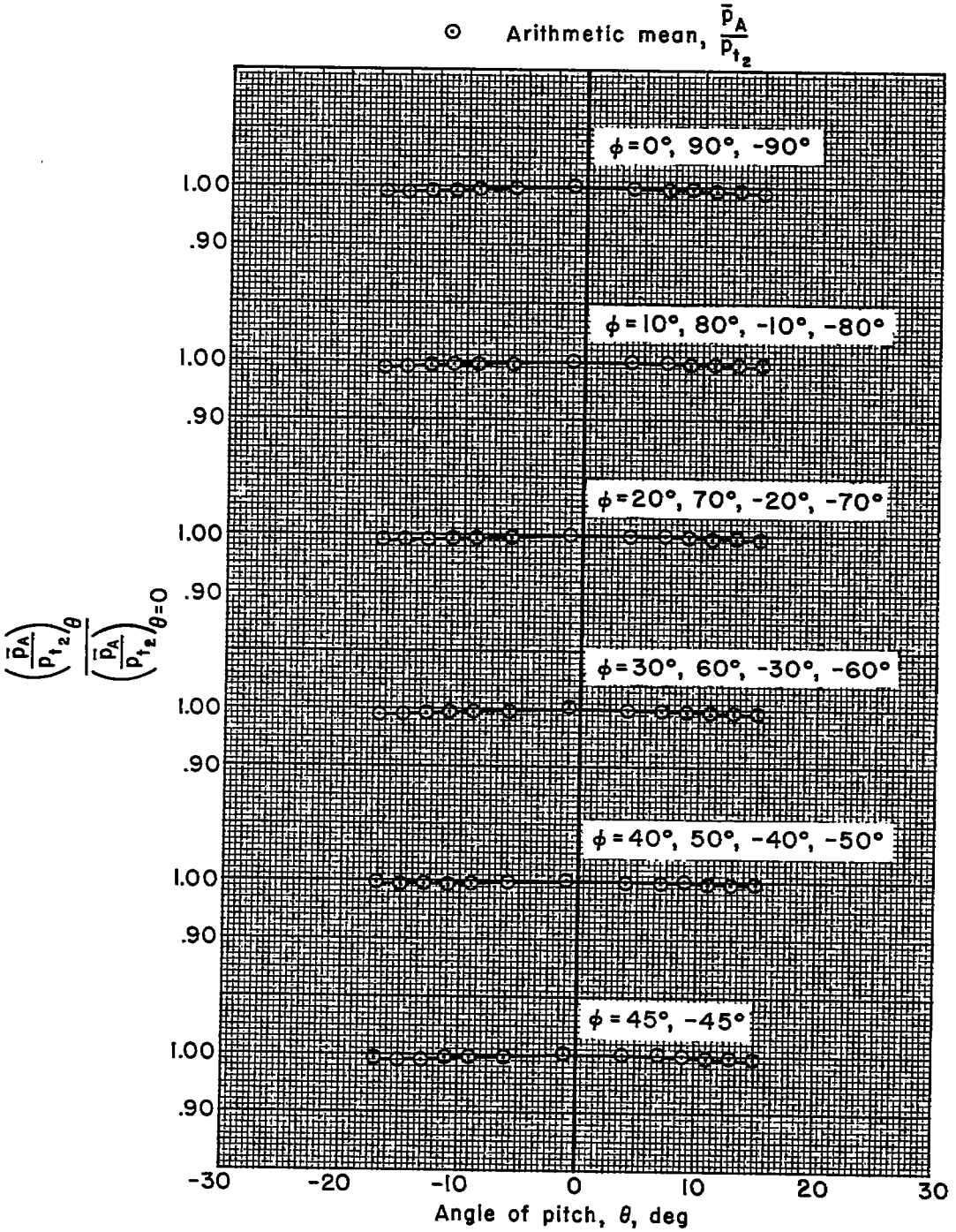

(a) M_1=1.72

Figure 6.—Effect of angle of pitch on ratio of average static pressure to pitot pressure.

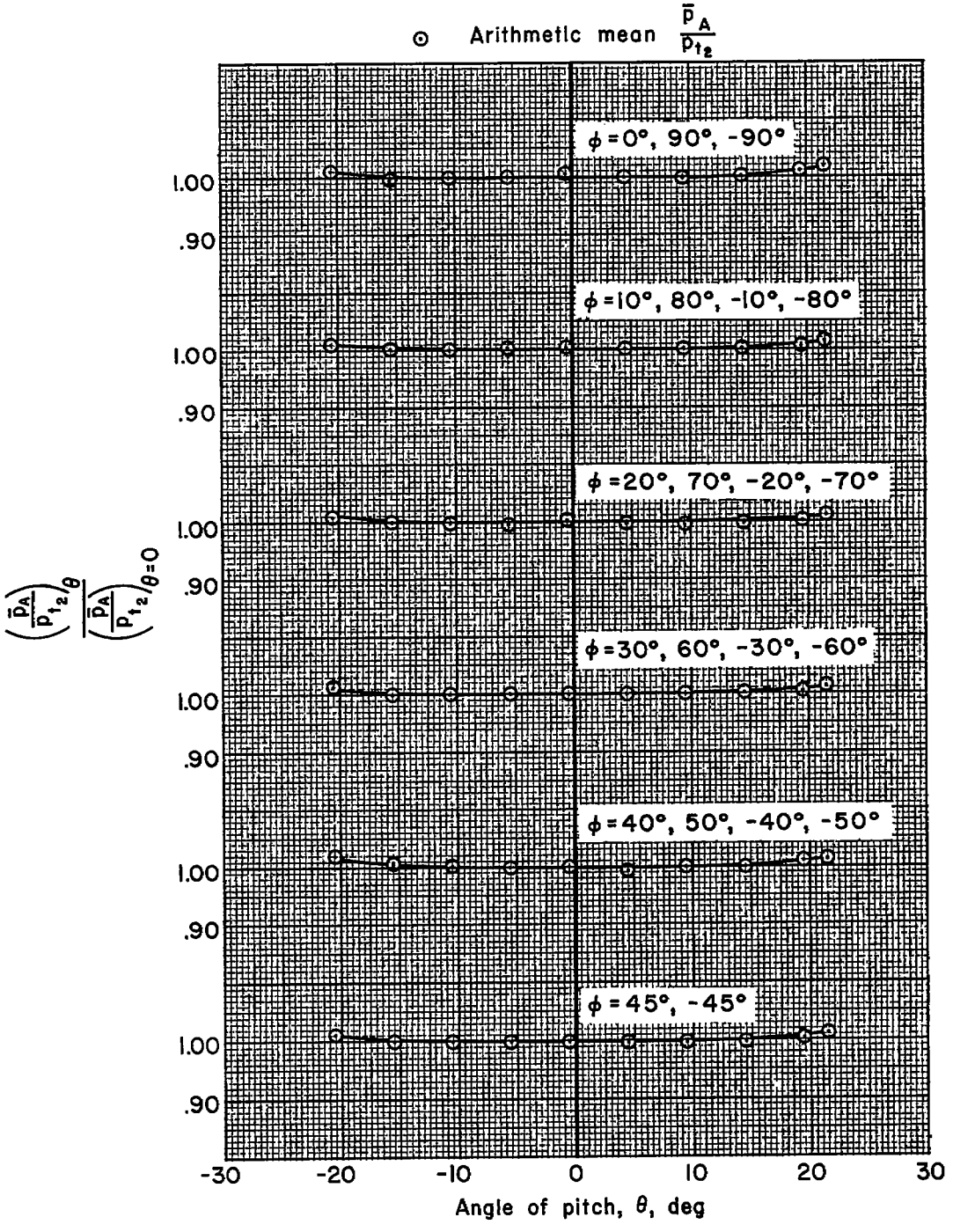

(b) M_1=1.95

Figure 6.- Continued.

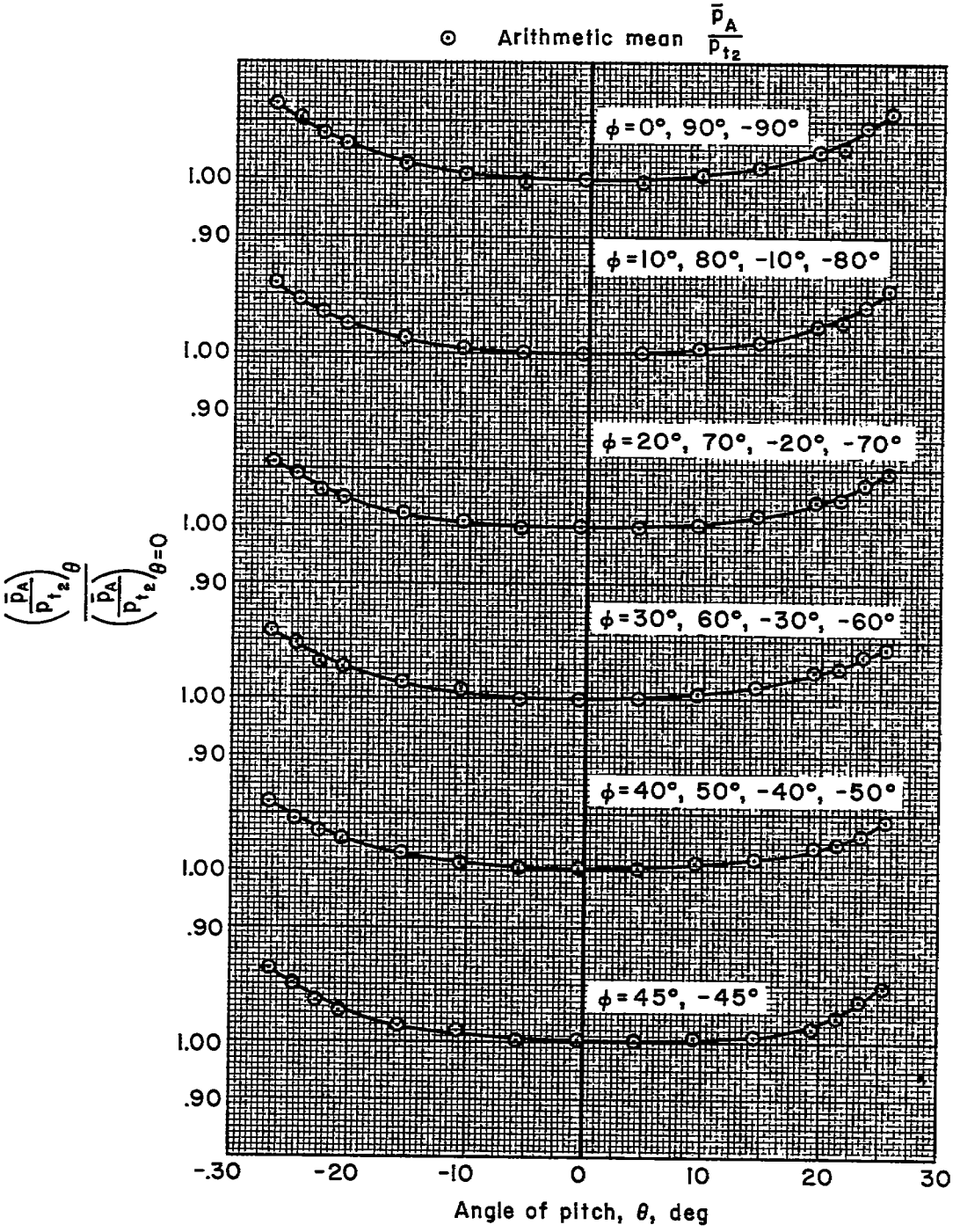

(c) $M_1 = 2.46$

Figure 6.– Concluded.

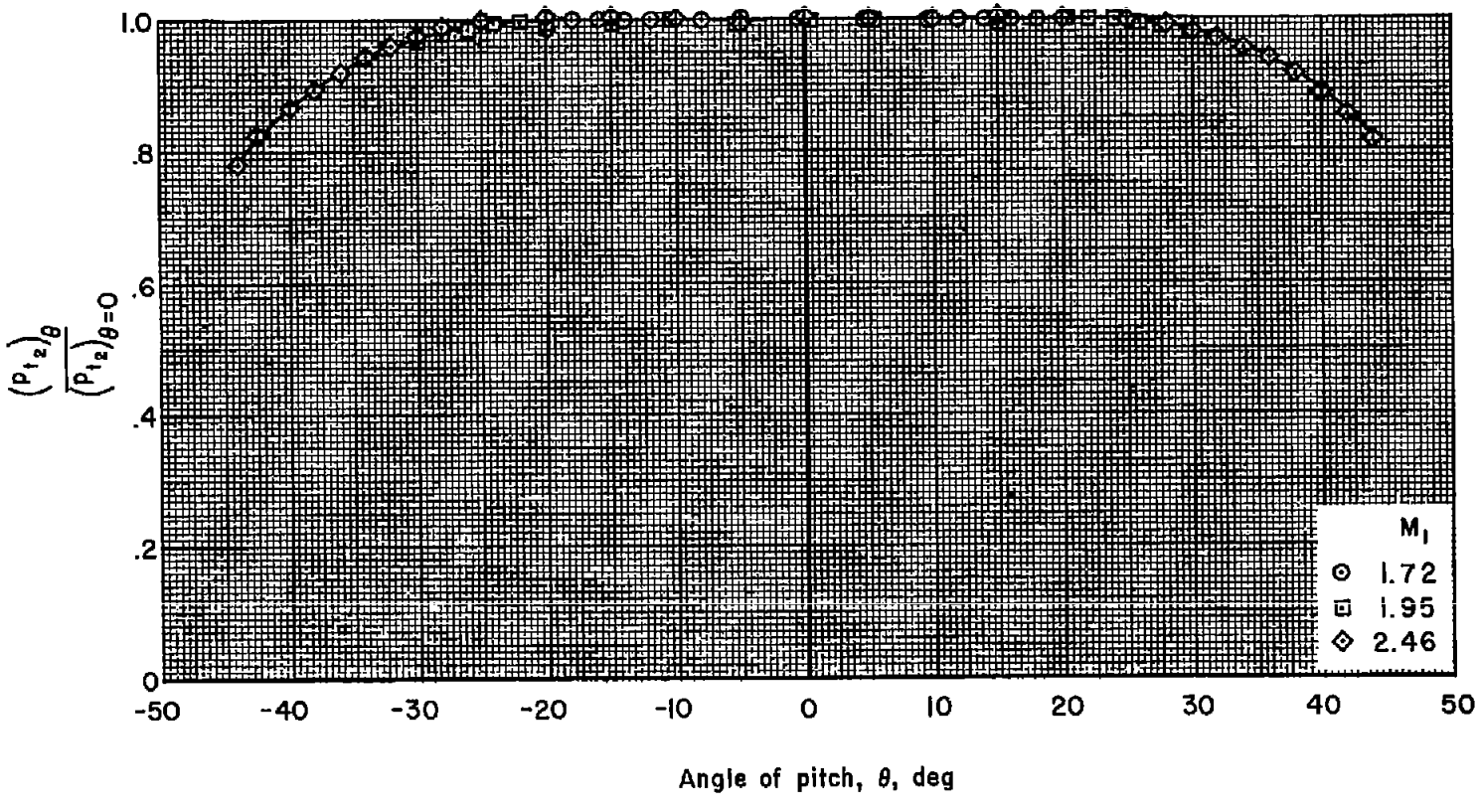

Figure 7.—Effect of angle of pitch on pitot pressure.

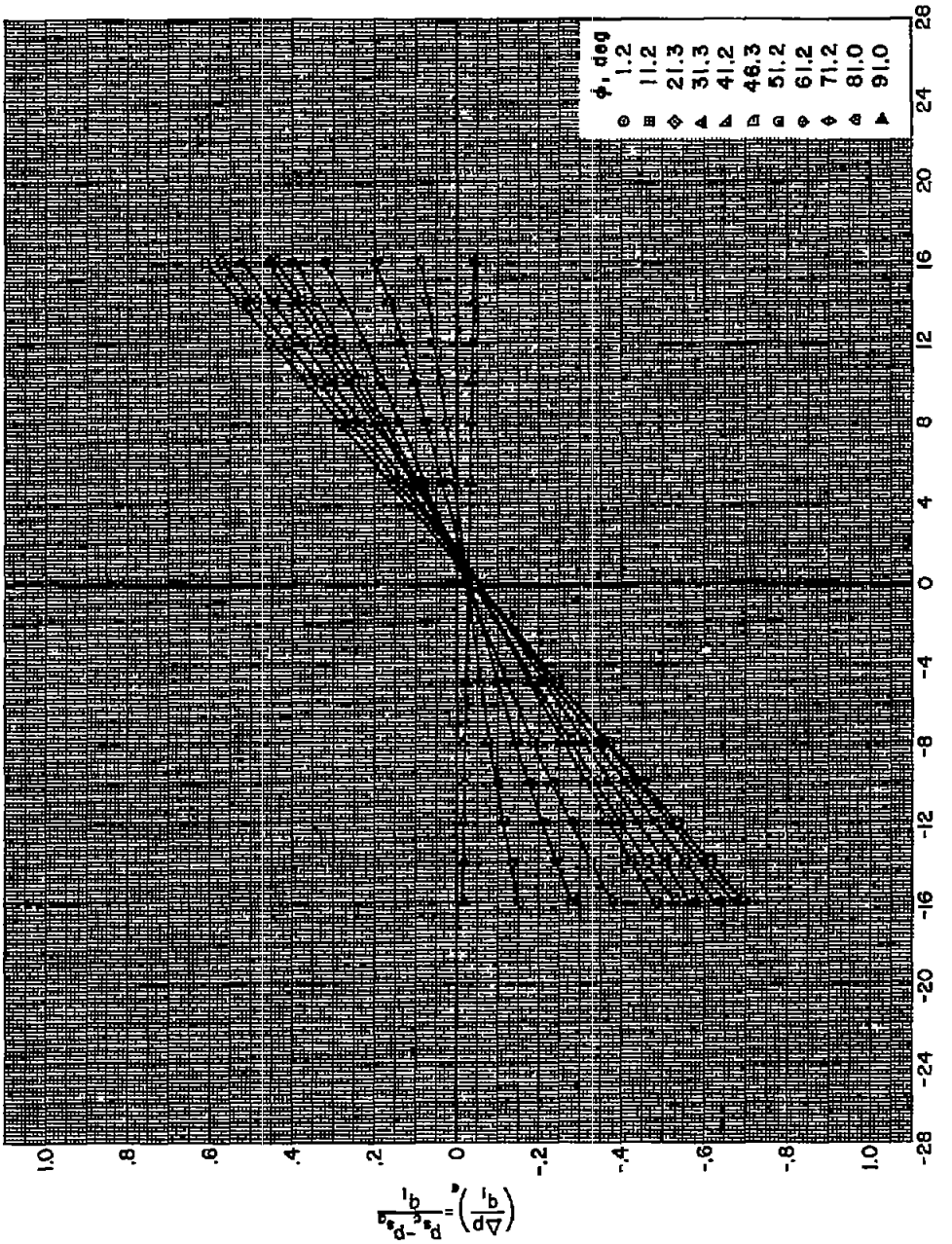

(a) $M_1=1.72$; orifices a and c.

Figure 8.–Variation of static pressure difference coefficient with angle of pitch.

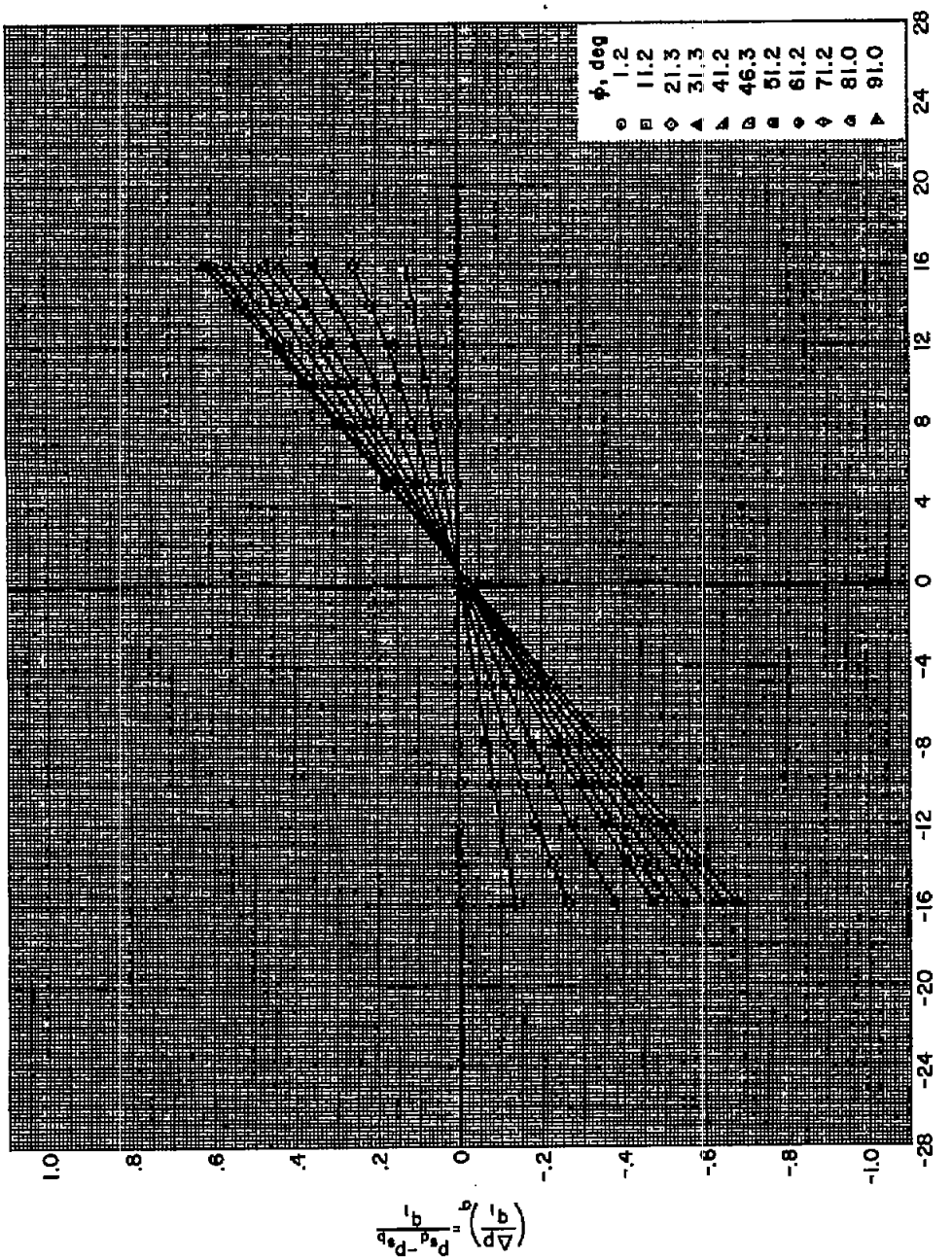

(b) M_1=1.72; orifices b and d.

Figure 8.—Continued.

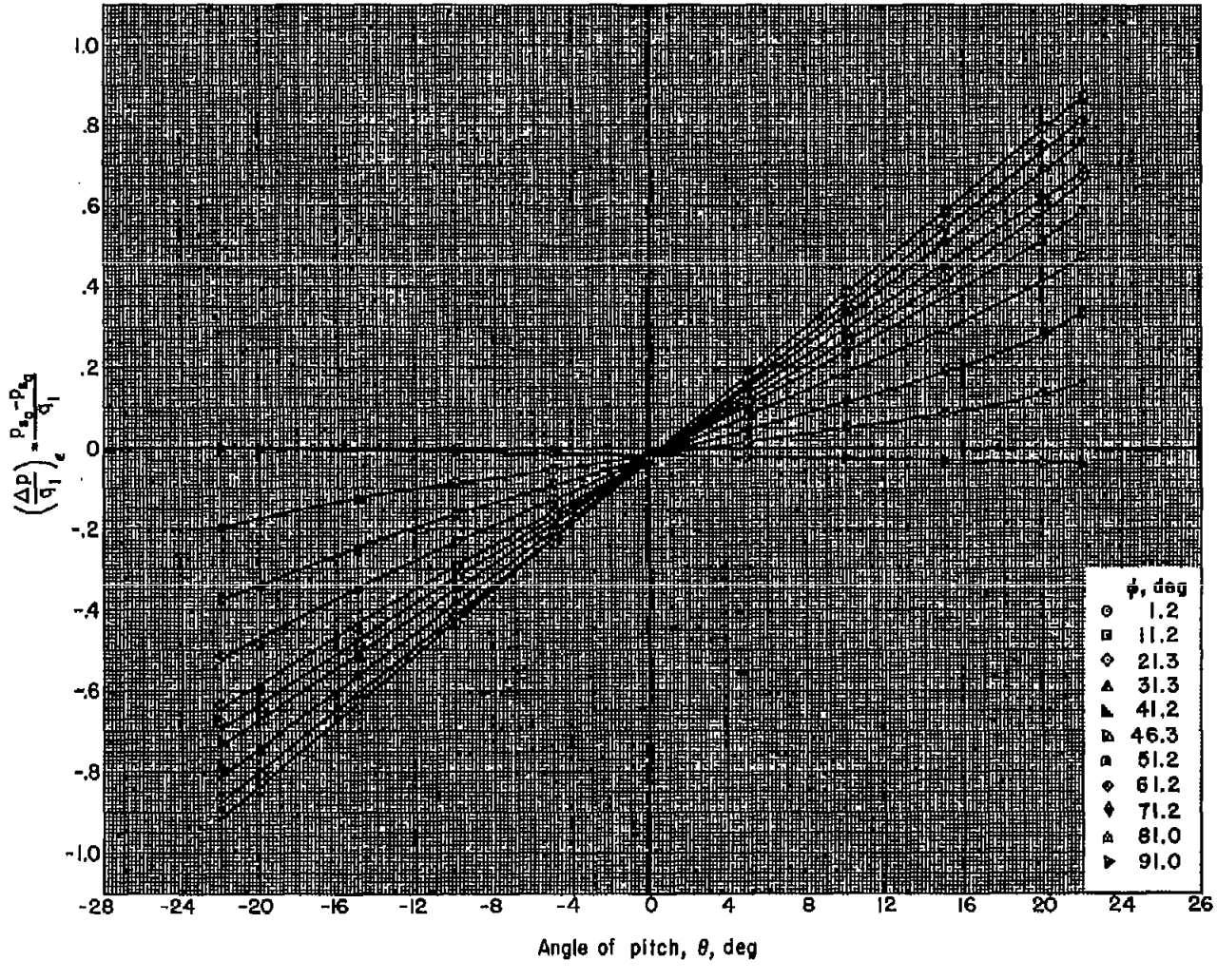

(c) $M_1 = 1.95$; orifices a and c.

Figure 8.–Continued.

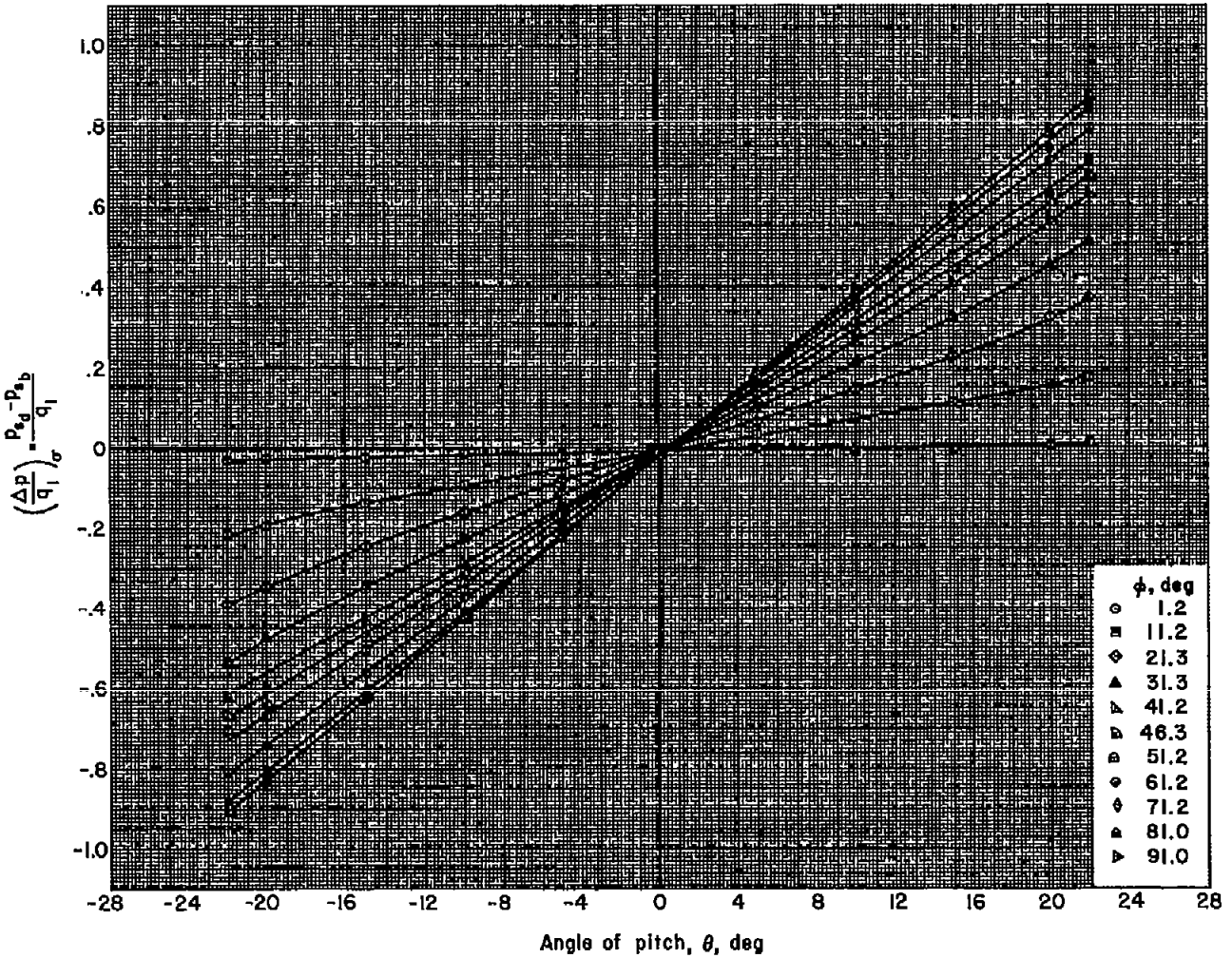

(d) $M_1 = 1.95$; orifices b and d.

Figure 8.—Continued.

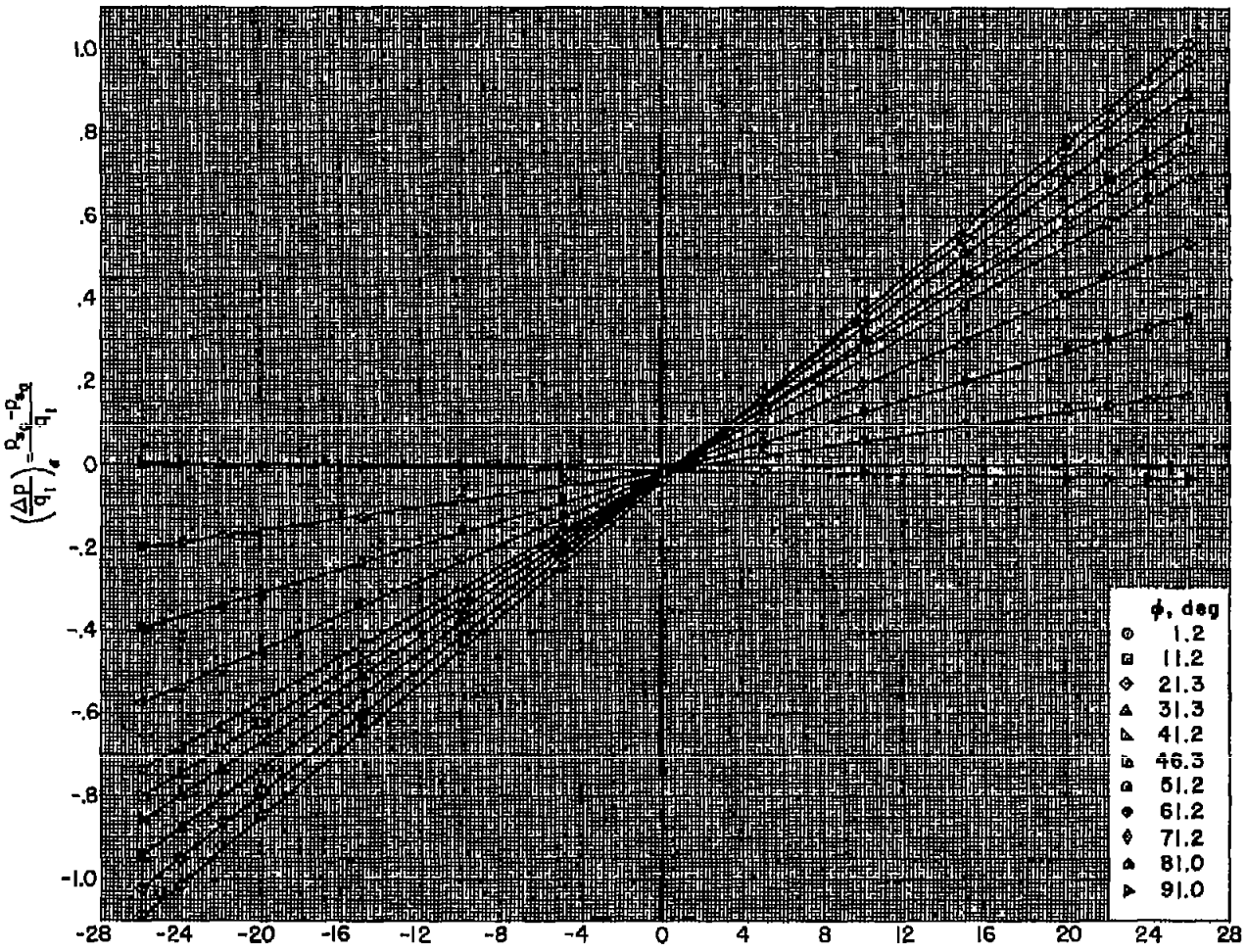

(e) $M_1 = 2.46$; orifices a and c.

Figure 8.–Continued.

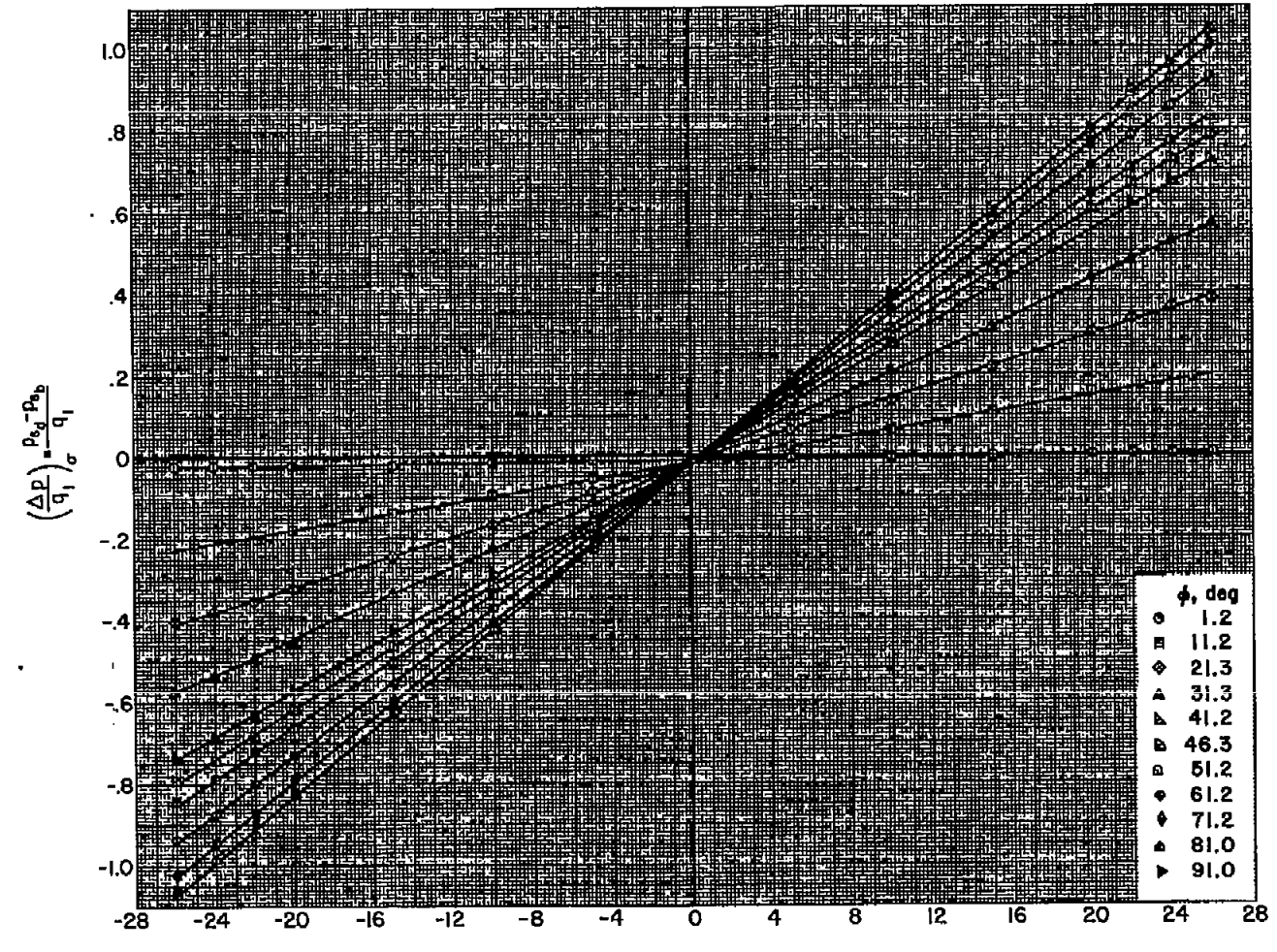

(f) $M_1 = 2.46$, orifices b and d.

Figure 8.–Concluded.

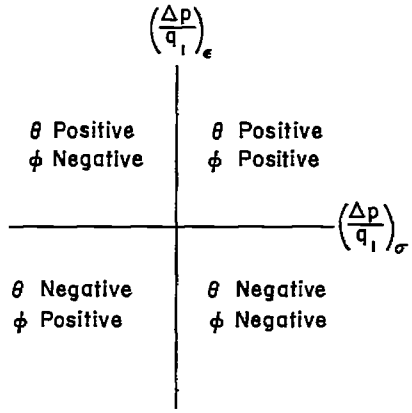

Sign convention

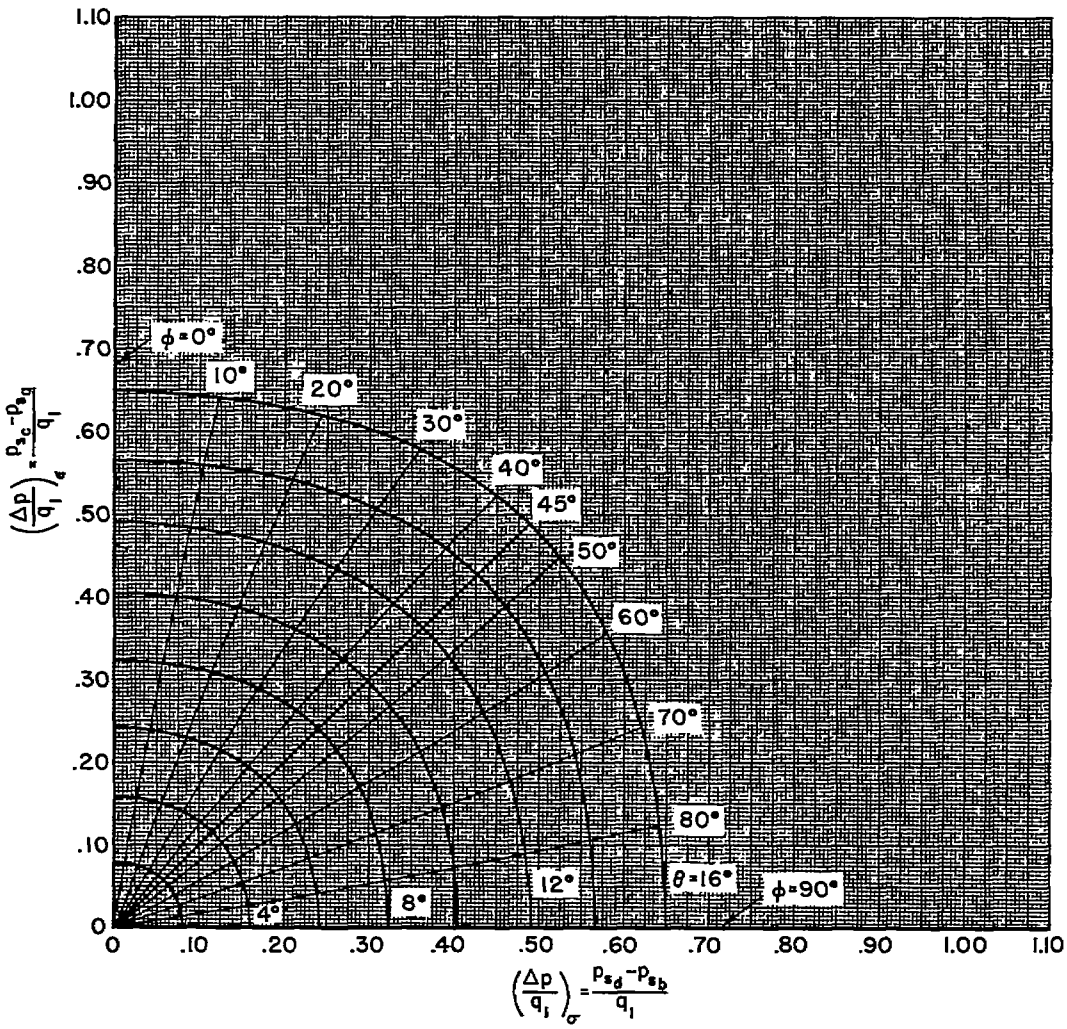

(a) M_1=1.72

Figure 9.–Chart for determination of pitch and roll angles.

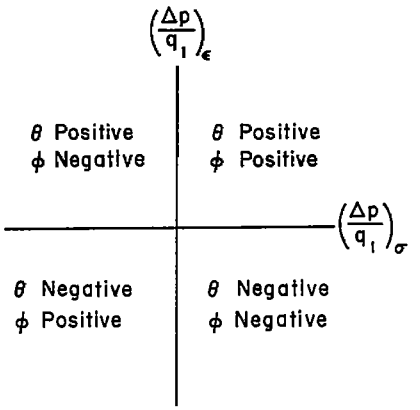

Sign convention

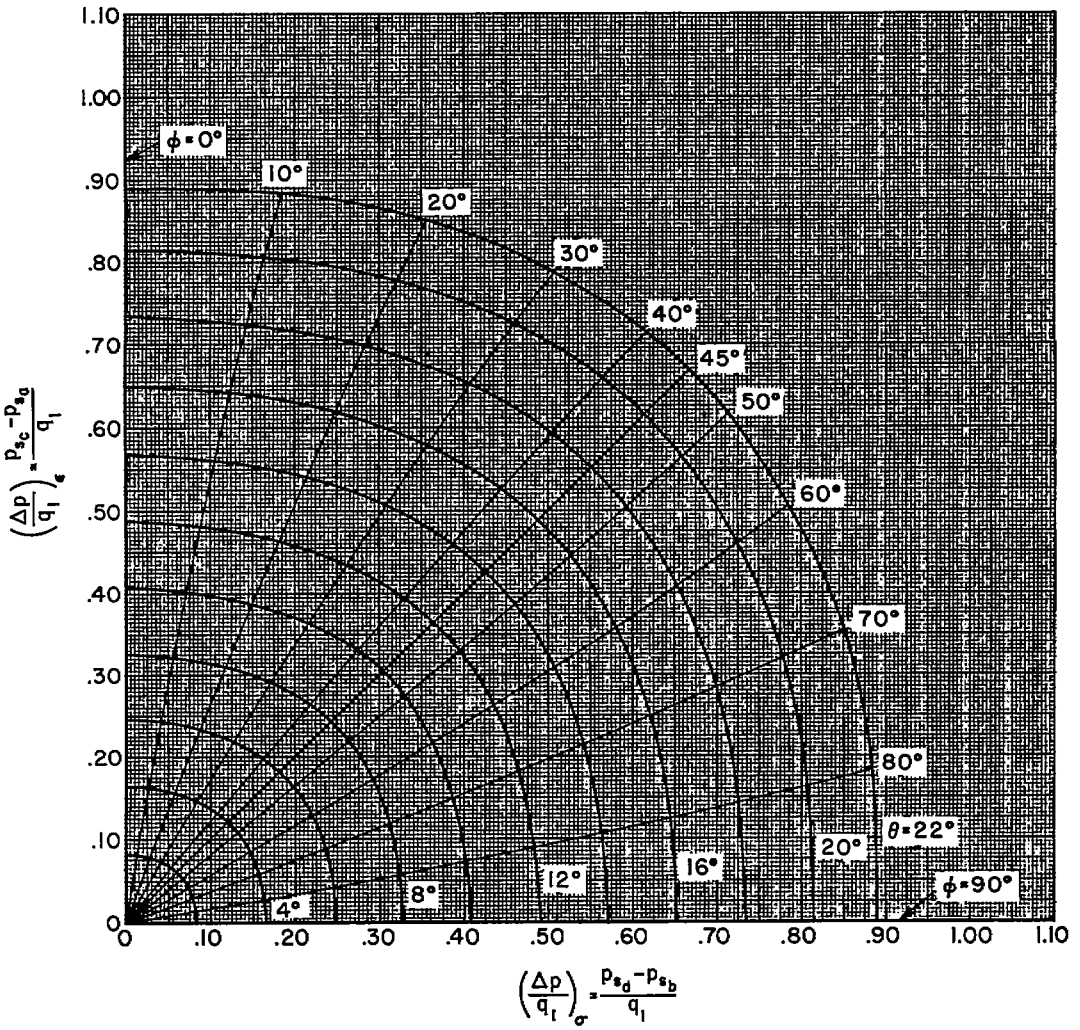

(b) $M_1 = 1.95$

Figure 9.– Continued.

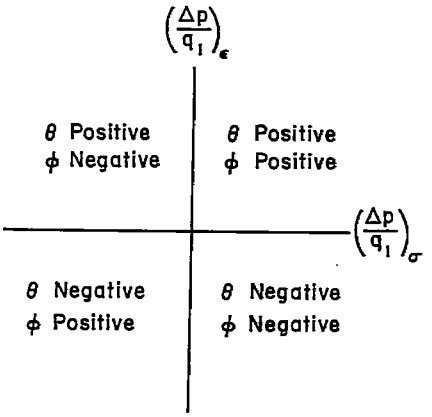

Sign convention

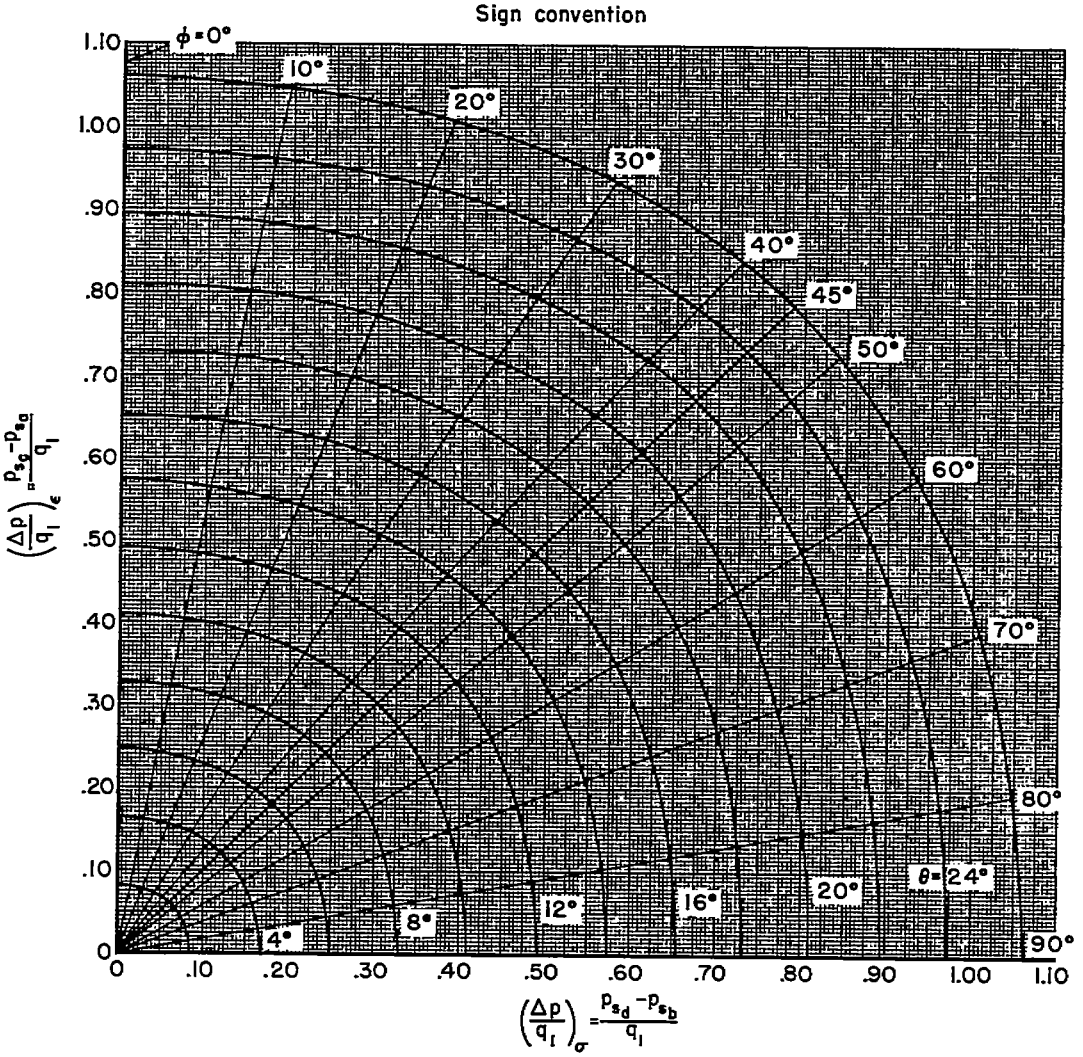

(c) $M_l = 2.46$

Figure 9.–Concluded.

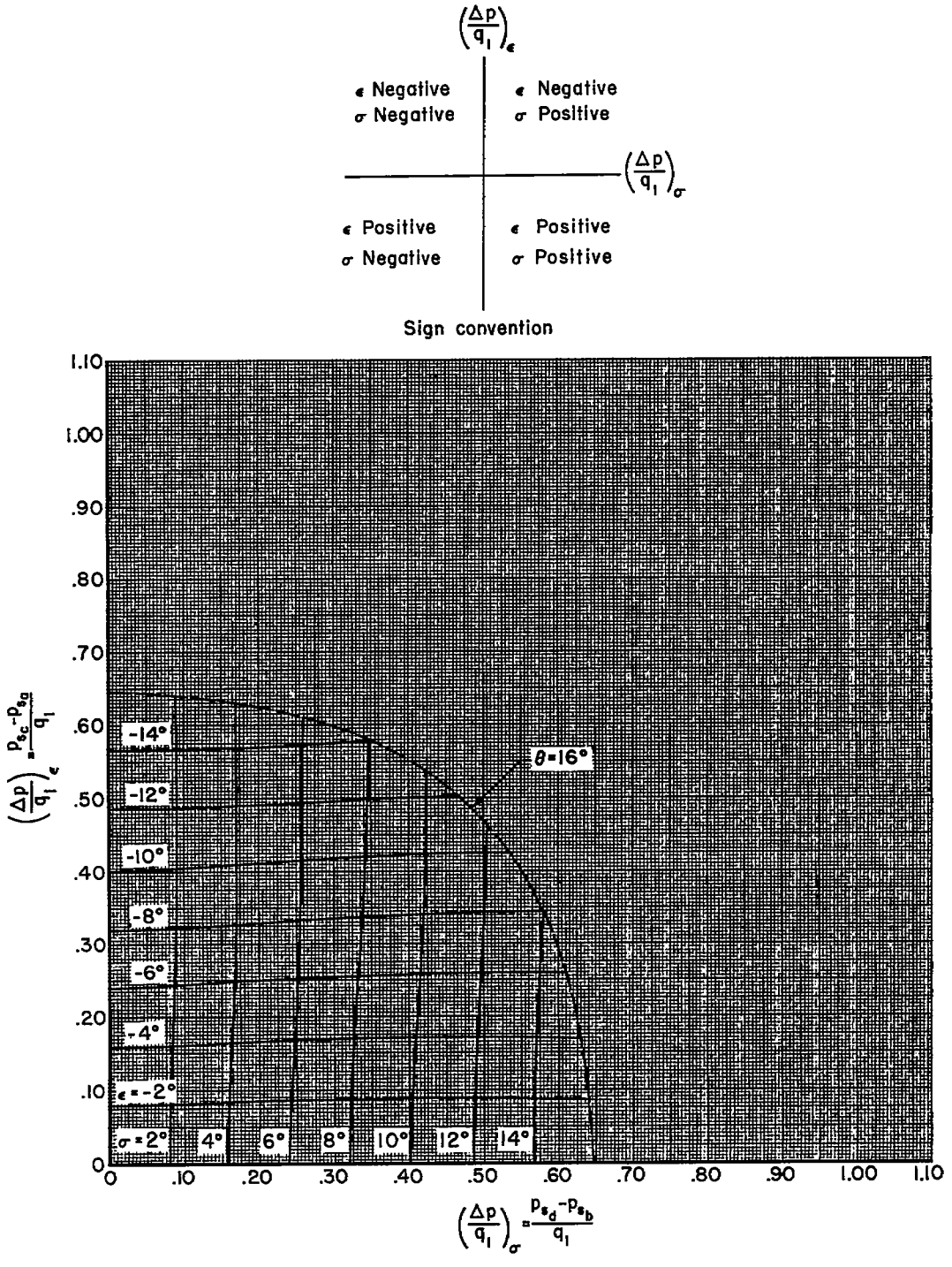

(a) $M_1 = 1.72$

Figure 10.– Chart for determination of downwash and sidewash angles.

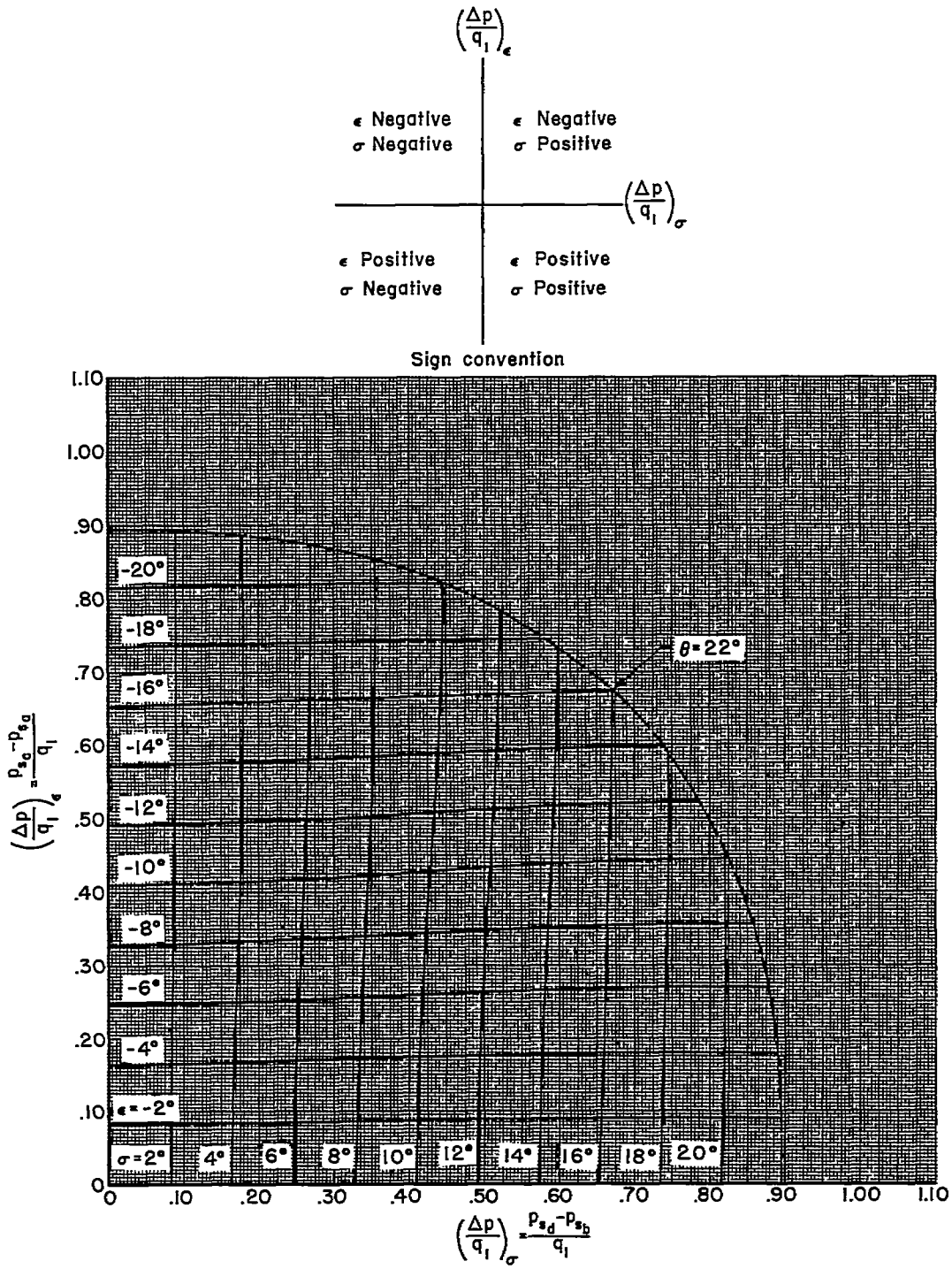

(b) $M_1 = 1.95$

Figure 10.—Continued.

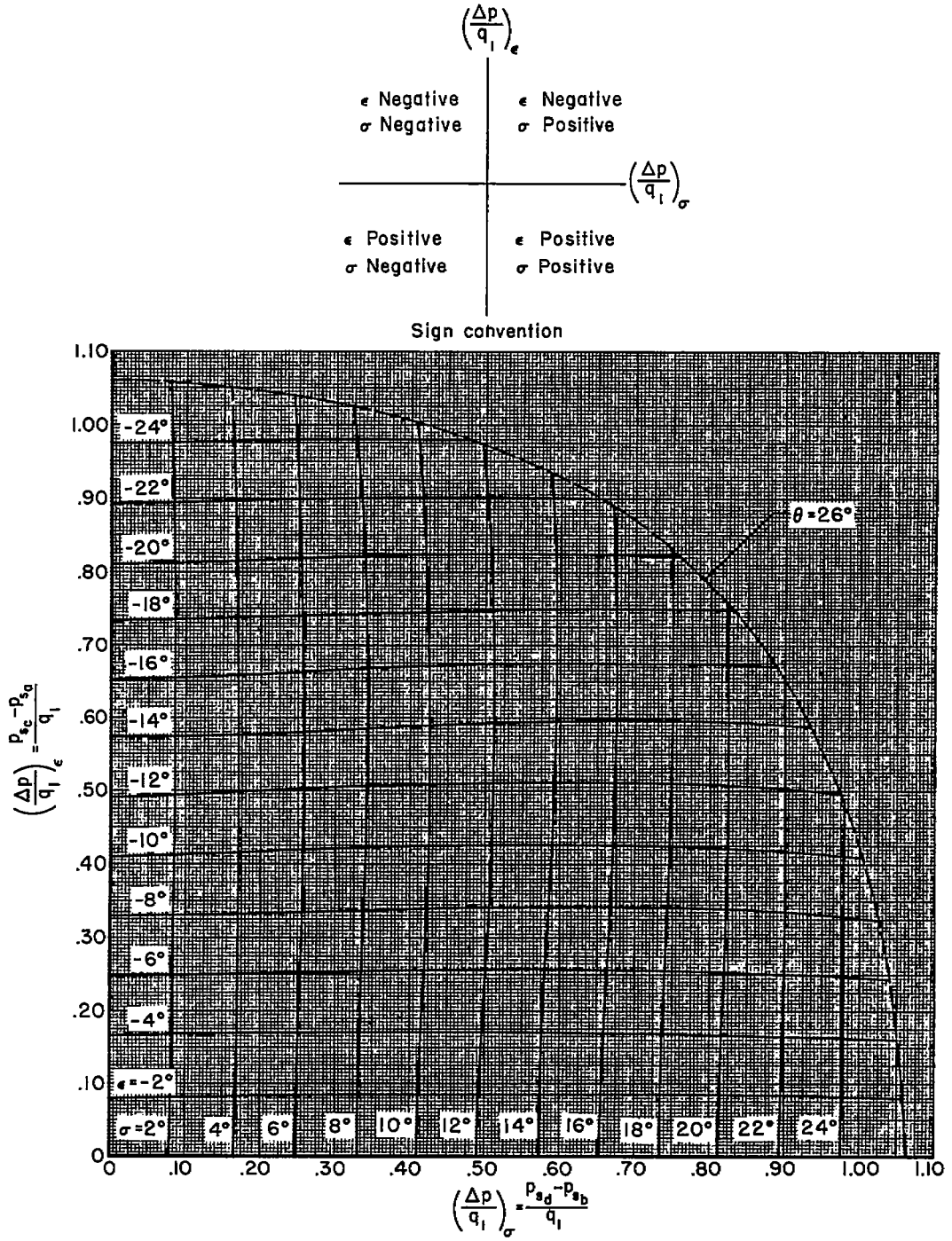

(c) $M_1 = 2.46$

Figure 10.- Concluded.